1

Introduction

Structure determination of almost any organic or biological molecule, as well as that of many inorganic molecules, begins with nuclear magnetic resonance (NMR) spectroscopy. During its existence of more than half a century, NMR spectroscopy has undergone several internal revolutions, repeatedly redefining itself as an increasingly complex and effective structural tool. Aside from X-ray crystallography, which can uncover the complete molecular structure of some pure crystalline materials, NMR spectroscopy is the chemist's most direct and general tool for identifying the structure of both pure compounds and mixtures, as either solids or liquids. The process often involves performing several NMR experiments to deduce the molecular structure from the magnetic properties of the atomic nuclei and the surrounding electrons.

1.1 Magnetic Properties of Nuclei

The simplest atom, hydrogen, is found in almost all organic compounds and is composed of a single proton and a single electron. The hydrogen atom is denoted as ^{1}H, in which the superscript signifies the sum of the atom's protons and neutrons, that is, the atomic mass of the element. For the purpose of NMR, the key aspect of the hydrogen nucleus is its angular momentum properties, which resemble those of a classical spinning particle. Because the spinning hydrogen nucleus is positively charged, it generates a magnetic field and possesses a *magnetic moment* $\boldsymbol{\mu}$, just as a charge moving in a circle creates a magnetic field (Figure 1.1). The magnetic moment $\boldsymbol{\mu}$ is a vector, because it has both magnitude and direction, as defined by its axis of spin in the figure. In this context, *boldface* symbols connote a vectorial parameter; when only the magnitude is under consideration, the symbol is depicted without boldface, as μ. The NMR experiment exploits the magnetic properties of nuclei to provide information on the molecular structure.

The spin properties of protons and neutrons in the nuclei of heavier elements combine to define the overall spin of the nucleus. When both the atomic number (the number of protons) and the atomic mass (the sum of the protons and neutrons) are even, the nucleus has no magnetic properties, as signified by a zero value of its *spin quantum number*, I (Figure 1.2). Such nuclei are considered not to be spinning. Common nonmagnetic (nonspinning) nuclei are carbon (^{12}C) and oxygen (^{16}O), which therefore are invisible to the NMR experiment. When either the atomic number or the atomic mass is odd, or when both are odd, the nucleus has magnetic properties that correspond to spin.

Nuclear Magnetic Resonance Spectroscopy: An Introduction to Principles, Applications, and Experimental Methods, Second Edition. Joseph B. Lambert, Eugene P. Mazzola, and Clark D. Ridge.

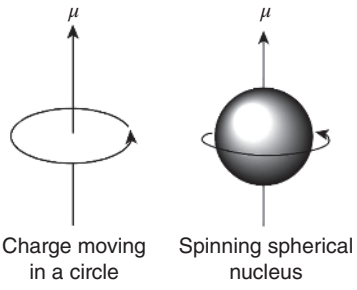

Figure 1.1 Analogy between a charge moving in a circle and a spinning nucleus.

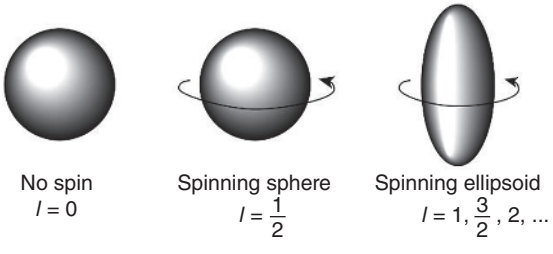

Figure 1.2 Three classes of nuclei.

For spinning nuclei, the spin quantum number can take on only certain values, which is to say that it is quantized. Those nuclei with a spherical shape have a spin I of ½, and those with a nonspherical, or quadrupolar, shape have a spin of 1 or more (in increments of ½).

Common nuclei with a spin of ½ include ^{1}H, ^{13}C, ^{15}N, ^{19}F, ^{29}Si, and ^{31}P. Thus, many of the most common elements found in organic molecules (H, C, N, P) have at least one isotope with $I = ½$ (although oxygen does not). The class of nuclei with $I = ½$ is the most easily examined by the NMR experiment. *Quadrupolar nuclei* ($I > ½$) include ^{2}H, ^{11}B, ^{14}N, ^{17}O, ^{33}S, and ^{35}Cl.

The magnitude of the magnetic moment produced by a spinning nucleus varies from atom to atom in accordance with the equation $\mu = \gamma \hbar I$ (see Appendix A for a derivation of this equation). The quantity $\hbar$ is Planck's constant h divided by 2π, and γ is a characteristic of the nucleus called the *gyromagnetic* or the *magnetogyric ratio*. The larger the gyromagnetic ratio, the larger is the magnetic moment of the nucleus. Nuclei that have the same number of protons, but different numbers of neutrons, are called *isotopes* (^{1}H/^{2}H, ^{14}N/^{15}N). The term *nuclide* generally is applied to any atomic nucleus.

To study nuclear magnetic properties, the experimentalist subjects nuclei to a strong laboratory magnetic field B_0 with units of tesla, or T ($1\,\text{T} = 10^4$ Gauss, or G). In the absence of the laboratory field, nuclear magnets of the same isotope have the same energy. When the B_0 field is turned on along a direction designated as the z-axis, the energies of the nuclei in a sample are affected. There is a slight tendency for magnetic moments to move along the general direction of B_0 ($+z$) rather than the opposite direction ($-z$). (This motion will be more fully described presently.) Nuclei with a spin of ½ assume only these two modes of motion. The splitting of spins into specific groups has been called the *Zeeman effect*.

The interaction is illustrated in Figure 1.3. At the left is a magnetic moment with a $+z$ component, and at the right is one with a $-z$ component. The nuclear magnets are

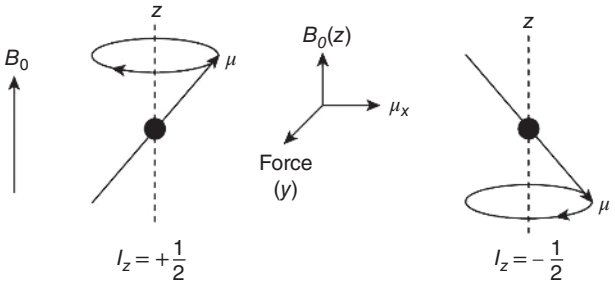

Figure 1.3 Interaction between a spinning nucleus and an external magnetic field B_0.

not actually lined up parallel to the $+z$ or $-z$ direction. Rather, the force of B_0 causes the magnetic moment to move in a circular fashion about the $+z$ direction in the first case and about the $-z$ direction in the second. In terms of vector analysis, the B_0 field in the z-direction operates on the x component of μ to create a force in the y-direction (Figure 1.3, inset in the middle). The force $\boldsymbol{F}$ is the cross, or vector, product between the magnetic moment $\boldsymbol{\mu}$ and the magnetic field $\boldsymbol{B}$ (a vector with magnitude only in the z-direction at this stage with value B_0), that is, $\boldsymbol{F} = \boldsymbol{\mu} \times \boldsymbol{B}$. The nuclear moment then begins to move toward the y-direction. Because the force of B_0 on μ, is always perpendicular to both B_0 and μ (according to the definition of a cross product), the motion of μ describes a circular orbit around the $+z$ or the $-z$-direction, in complete analogy to the forces present in a spinning top or gyroscope. This motion is termed *precession*.

As the process of quantization allows only two directions of precession for a spin-½ nucleus (Figure 1.3), two assemblages or *spin states* are created, designated as $I_z = +½$ for those precessing with the field ($+z$) and $I_z = -½$ for those precessing against the field ($-z$) (some texts refer to the quantum number I_z as m_I). The assignment of signs (+ or −) is entirely arbitrary. The designation $I_z = +½$ is given to the slightly lower energy. In the absence of B_0, the precessional motions are absent, and all nuclei have the same energy.

The relative proportions of nuclei with $+z$ and $-z$ precession in the presence of B_0 is defined by Boltzmann's law (Eq. (1.1)),

$$\frac{n\left(+\frac{1}{2}\right)}{n\left(-\frac{1}{2}\right)} = \exp\left(\frac{\Delta E}{kT}\right) \tag{1.1}$$

in which n is the population of a spin state, k is Boltzmann's constant, T is the absolute temperature in kelvin (K), and ΔE is the energy difference between the spin states. Figure 1.4a depicts the energies of the two states and the difference ΔE between them.

The precessional motion of the magnetic moment around B_0 occurs with angular frequency ω_0, called the *Larmor frequency*, whose units are radians per second (rad s^{-1}). As B_0 increases, so does the angular frequency, that is, $\omega_0 \propto B_0$, as is demonstrated in Appendix A. The constant of proportionality between ω_0 and B_0 is the gyromagnetic ratio γ, so that $\omega_0 = \gamma B_0$. The natural precession frequency can be expressed as linear frequency in Planck's relationship $\Delta E = h\nu_0$, or as angular frequency $\Delta E = \hbar\omega_0$

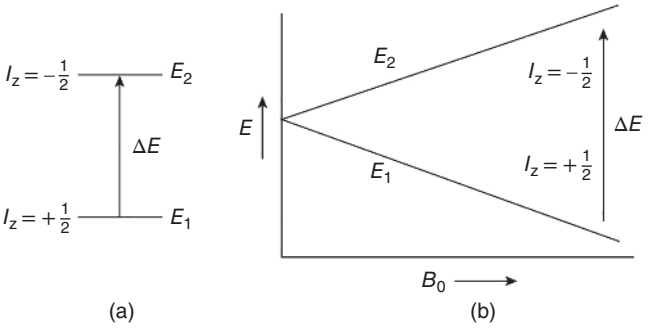

Figure 1.4 (a) The energy difference between spin states. (b) The energy difference as a function of the external field B_0.

($\omega_0 = 2\pi\nu_0$). In this way, the energy difference between the spin states is related to the Larmor frequency by the formula of Eq. (1.2).

$$\Delta E = \hbar\omega_0 = h\nu_0 = \gamma\hbar B_0 \tag{1.2}$$

Thus, as the B_0 field increases, the difference in energy between the two spin states increases, as illustrated in Figure 1.4b. Appendix A provides a complete derivation of these relationships.

The foregoing equations indicate that the natural precession frequency of a spinning nucleus ($\omega_0 = \gamma B_0$) depends only on the nuclear properties contained in the gyromagnetic ratio γ and on the laboratory-determined value of the magnetic field B_0. For a proton in a magnetic field B_0 of 7.05 T, the frequency of precession is 300 MHz, and the difference in energy between the spin states is only 0.0286 cal mol^{-1} (0.120 J mol^{-1}). This value is extremely small in comparison with the energy differences between vibrational or electronic states. At a higher field, such as 14.1 T, the frequency increases proportionately to 600 MHz in this case.

In the NMR experiment, the two states illustrated in Figure 1.4 are made to interconvert by applying a second magnetic field B_1 at radio frequency (RF) range. When the frequency of the B_1 field is the same as the Larmor frequency of the nucleus, energy can flow by absorption and emission between this newly applied field and the nuclei. Absorption of energy occurs as $+\frac{1}{2}$ nuclei become $-\frac{1}{2}$ nuclei, and emission occurs as $-\frac{1}{2}$ nuclei become $+\frac{1}{2}$ nuclei. Since there is an excess of $+\frac{1}{2}$ nuclei at the beginning of the experiment, there is a net absorption of energy. The process is called *resonance*, and the absorption may be detected electronically and displayed as a plot of frequency vs amount of energy absorbed. Because the resonance frequency ν_0 is highly dependent on the structural environment of the nucleus, NMR spectroscopy has become the structural tool of choice for chemists. Figure 1.5 illustrates the NMR spectrum for the protons in benzene. Absorption is represented by a peak directed upward from the baseline.

Because gyromagnetic ratios vary among elements and even among isotopes of a single element, resonance frequencies also vary ($\omega_0 = \gamma B_0$). There is essentially no overlap in the resonance frequencies of different nuclides, including isotopes. At the field strength at which protons resonate at 300 MHz (7.05 T), ^{13}C nuclei resonate at 75.45 MHz, ^{15}N nuclei at 30.42 MHz, and so on. At 14.1 T, the frequencies would be doubled, respectively, 600, 150.9, and 60.84 MHz.

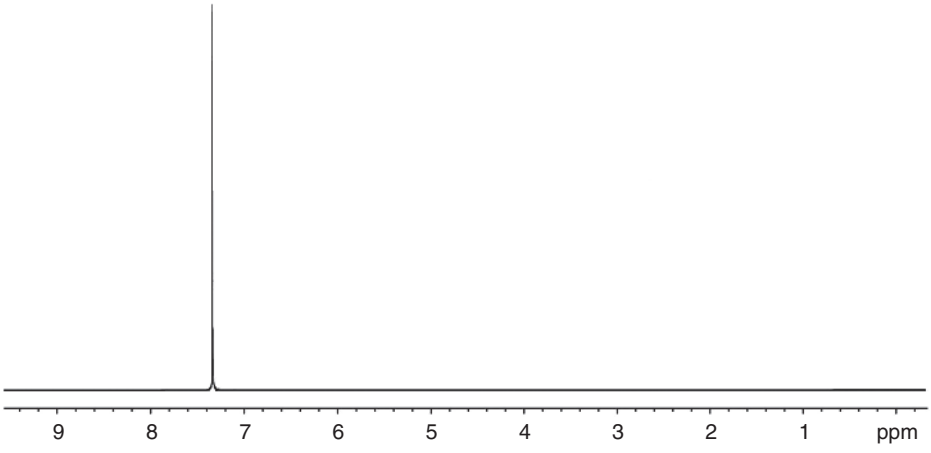

Figure 1.5 The 300 MHz ^{1}H spectrum of benzene.

The magnitude of the gyromagnetic ratio γ also has an important influence on the intensity of the resonance. The difference in energy, $\Delta E = \gamma \hbar B_0$ (Eq. (1.2)), between the two spin states is directly proportional not only to B_0, as illustrated in Figure 1.4b, but also to γ. From Boltzmann's law (Eq. (1.1)), when ΔE is larger, there is a greater population difference between the two states. A greater excess of $I_z = +½$ spins (designated the E_1 state) means that more nuclei are available to flip to the E_2 state with $I_z = -½$, so the resonance intensity is larger. The proton has one of the largest gyromagnetic ratios, so its spin states are relatively far apart, and the value of ΔE is especially large. The proton signal, consequently, is very strong. Many other important nuclei, such as ^{13}C and ^{15}N, have much smaller gyromagnetic ratios and hence have smaller differences between the energies of the two spin states (Figure 1.6). Thus, their signals are much less intense.

When spins have values greater than ½, more than two spin states are allowed. For $I = 1$ nuclei, such as ^{2}H and ^{14}N, the magnetic moments may precess about three directions relative to B_0: parallel ($I_z = +1$), perpendicular (0), and opposite (-1). In general, there are $(2I + 1)$ spin states—for example, six for $I = 5/2$ (^{17}O has this spin). The values

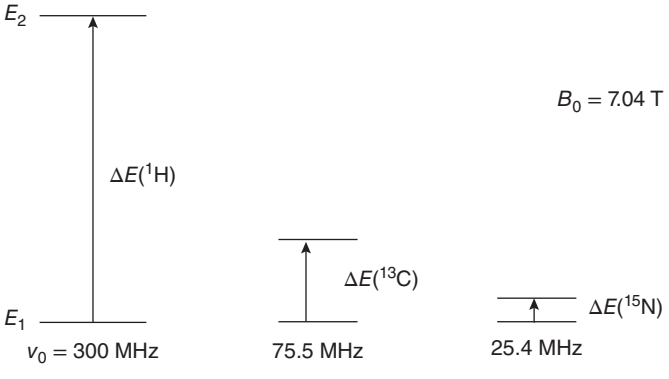

Figure 1.6 The energy difference between spin states for three nuclides with various relative magnitudes of the gyromagnetic ratio ($|\gamma|$): 26.75 for ^{1}H, 6.73 for ^{13}C, and 2.71 for ^{15}N.

of I_z extend from $+I$ to $-I$ in increments of 1 ($+I$, $(+I-1)$, $(+I-2)$, …, $-I$). For example, $I_z = +1$, 0, and -1 for $I = 1$, and $+3/2$, $+½$, $-½$, and $-3/2$ for $I = 3/2$. Hence, the energy state picture is more complex for quadrupolar than for spherical nuclei.

In summary, the NMR experiment consists of immersing magnetic nuclei in a strong field B_0 to distinguish them according to their values of I_z ($+½$ and $-½$ for spin-½ nuclei), followed by the application of a B_1 field whose frequency corresponds to the Larmor frequency of the nuclei under examination ($\omega_0 = \gamma B_0$). This application of energy results in a net absorption, as the excess $+½$ nuclei are converted to $-½$ nuclei. The resonance frequency varies from nuclide to nuclide according to the value of the gyromagnetic ratio γ. The energy difference between the I_z spin states, $\Delta E = h\nu$, which determines the intensity of the absorption, depends on the value of B_0 (Figure 1.4) and on the gyromagnetic ratio of the nucleus ($\Delta E = \gamma \hbar B_0$) (Figure 1.6).

1.2 The Chemical Shift

The remaining sections in this chapter discuss the various factors that determine the content of NMR spectra. Uppermost is the location of the resonance in the spectrum, the so-called resonance frequency ν_0 (or ω_0 as angular frequency), which depends on the molecular environment as well as on γ and B_0 ($\nu_0 = \gamma B_0/2\pi$ or $\omega_0 = \gamma B_0$). This dependence of the resonance frequency on structure is the ultimate reason for the importance of NMR spectroscopy in chemistry.

The electron cloud that surrounds the nucleus also has charge, motion, and, hence, a magnetic moment. The magnetic field generated by the electrons alters the B_0 field in the microenvironment around the nucleus. The actual field present at a given nucleus thus depends on the nature of the surrounding electrons. This electronic modulation of the B_0 field is termed *shielding* and is represented quantitatively by the Greek letter sigma (σ). The actual field at the nucleus becomes B_{local} and may be expressed as $B_{\text{local}} = B_0(1-\sigma)$, in which the electronic shielding σ is positive for protons. The variation of the resonance frequency with shielding has been termed the *chemical shift*.

By substituting B_{local} for B_0 in Eq. (1.2), the expression for the resonance frequency in terms of shielding becomes Eq. (1.3).

$$\nu_0 = \frac{\gamma B_0(1-\sigma)}{2\pi} \tag{1.3}$$

Decreased shielding thus results in a higher resonance frequency ν_0 at constant B_0, since σ enters the equation after a negative sign. For example, the presence of an electron-withdrawing group in a molecule reduces the electron density around a proton so that there is less shielding and, consequently, a higher resonance frequency than in the case of a molecule that lacks the electron-withdrawing group. Hence, protons in fluoromethane (CH_3F) resonate at a higher frequency than those in methane (CH_4), because the fluorine atom withdraws electrons from around the hydrogen nuclei.

Figure 1.7 separately shows the NMR spectra of the protons and the carbons of methyl acetate ($CH_3CO_2CH_3$). Although 98.9% of naturally occurring carbon is the nonmagnetic ^{12}C, the carbon NMR experiment is carried out on the 1.1% of ^{13}C, which has an I of ½. Because of differential electronic shielding, the ^1H spectrum contains separate resonances for the two types of protons (O—CH_3 and C—CH_3), and the ^{13}C spectrum

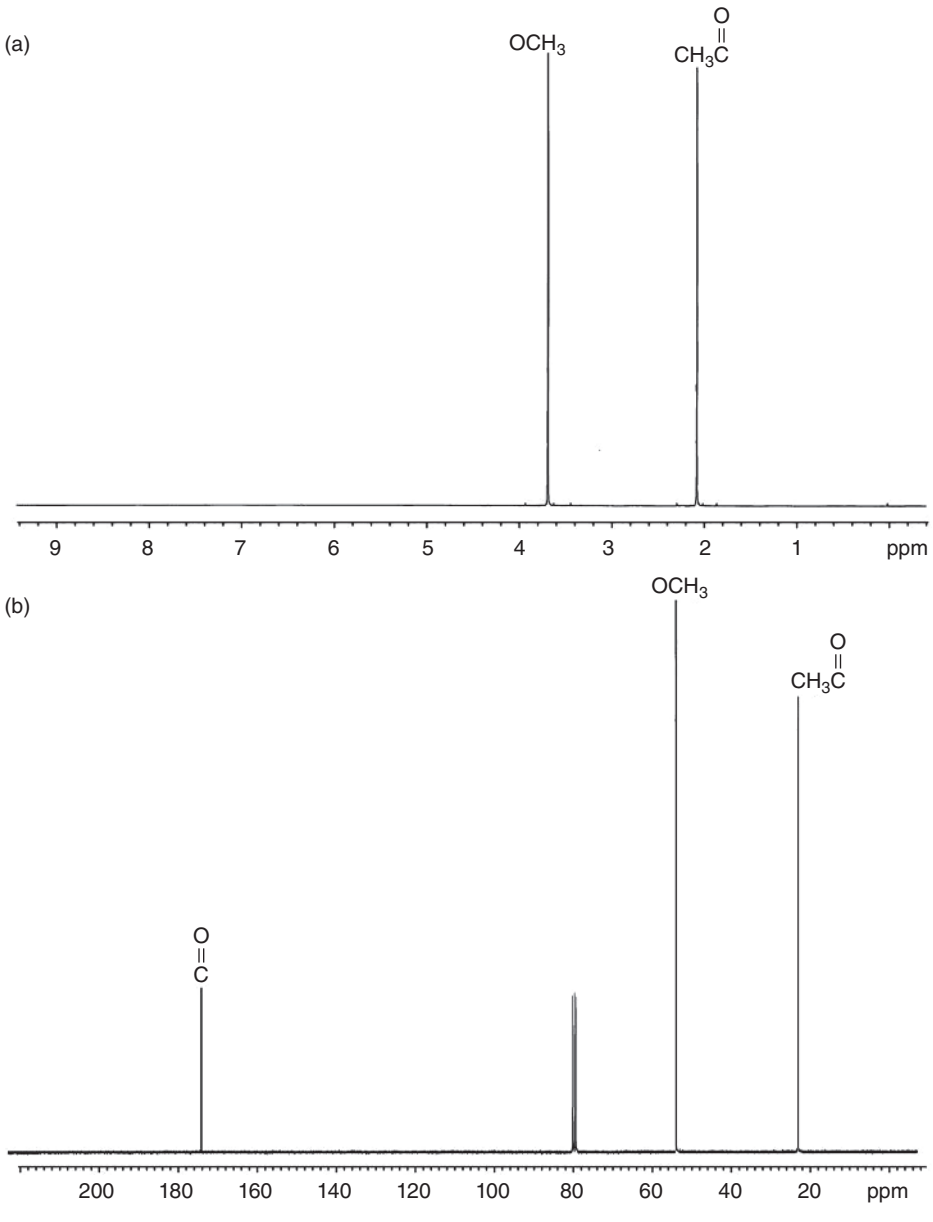

Figure 1.7 The 300 MHz ^{1}H spectrum (a) and the 75.45 MHz ^{13}C spectrum (b) of methyl acetate in $CDCl_3$. The resonance at δ 77 is from the solvent. The ^{13}C spectrum has been decoupled from the protons.

contains separate resonances for the three types of carbons (O—CH_3, C—CH_3, and carbonyl) (Figure 1.8).

The proton resonances may be assigned on the basis of the electron-withdrawing abilities, or electronegativities, of the neighboring atoms. The ester oxygen is more electron withdrawing than the carbonyl group, so the O—CH_3 resonance occurs at a higher

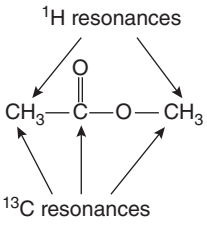

Figure 1.8 The resonances that are expected from methyl acetate.

frequency than (and to the left of) the C—CH_3 resonance. By convention, frequency in the spectrum increases from right to left, for consistency with other forms of spectroscopy. Therefore, shielding increases from left to right, because of the negative sign before σ in Eq. (1.3).

The system of units depicted in Figure 1.7 and used throughout this book has been developed to overcome the fact that chemical information often is found in small differences between large numbers. An intuitive system might be absolute frequency—for example, in hertz (Hz, which corresponds to cycles per second or cps). At the common field of 7.05 T, for instance, all protons resonate in the vicinity of 300 MHz. A scale involving numbers like 300.000 764, however, is cumbersome. Moreover, frequencies would vary from one B_0 field to another (Eq. (1.3)). Thus, for every element or isotope, a reference material has been chosen and assigned a relative frequency of zero. For both protons and carbons, the substance is tetramethylsilane [$(CH_3)_4Si$], usually called TMS, which is soluble in most organic solvents, is unreactive, has a strong signal, and is volatile. In addition, the low electronegativity of silicon means that the protons and carbons are surrounded by a relatively high density of electrons. Hence, they are highly shielded and resonate at very low frequency, to the right in the spectrum. Shielding by silicon is so strong, in fact, that the proton and carbon resonances of TMS are placed at the right extreme of the spectrum, providing a convenient spectral zero. In Figures 1.5 and 1.7, the position marked "0 ppm" is the hypothetical position of TMS.

The chemical shift may be expressed as the distance from a chemical reference standard by writing Eq. (1.3) twice—once for an arbitrary nucleus i as in Eq. (1.4a),

$$\nu_i = \frac{\gamma B_0(1-\sigma_i)}{2\pi} \tag{1.4a}$$

and again for the reference, that is, TMS, as Eq. (1.4b).

$$\nu_r = \frac{\gamma B_0(1-\sigma_r)}{2\pi} \tag{1.4b}$$

The distance between the resonances in the NMR frequency unit (Hz, which equals cps) then is given by the formula in Eq. (1.5).

$$\Delta\nu = \nu_i - \nu_r = \frac{\gamma B_0(\sigma_r - \sigma_i)}{2\pi} = \frac{\gamma B_0 \Delta\sigma}{2\pi} \tag{1.5}$$

This expression for the frequency differences still depends on the magnetic field B_0. In order to have a common unit at all B_0 fields, the chemical shift of nucleus i is defined by Eq. (1.6),

$$\delta = \frac{\Delta\nu}{\nu_r} = \frac{\sigma_r - \sigma_i}{1-\sigma_r} \sim \sigma_r - \sigma_i, \tag{1.6}$$

in which the frequency difference in Hz (Eq. (1.5)) is divided by the reference frequency in MHz (Eq. (1.4b)). In this fashion, the constants including the field B_0 cancel out. The δ scale is thus in units of Hz/MHz or parts per million (ppm) of the field. Because the reference shielding is chosen to be much less than 1.0, that is, $(1 - \sigma_r) \sim 1$, δ corresponds to the differences in shielding of the reference and the nucleus. An increase in σ_i, therefore, results in a decrease in δ_i, in accordance with Eq. (1.6).

As seen in the ^{1}H spectrum of methyl acetate (Figure 1.7), the δ value for the C—CH_3 protons is 2.07 ppm (always written as "δ 2.07" without "ppm," which is understood) and that for the O—CH_3 protons is 3.67 ppm (δ 3.67). These values remain the same in spectra taken at any B_0 field, such as either 1.41 T (60 MHz) or 24.0 T (1020 MHz), which represent the extremes of spectrometers currently in use. Chemical shifts expressed in Hz, however, vary from field to field. Thus, a resonance that is 90 Hz from TMS at 60 MHz is 450 Hz from TMS at 300 MHz, but always has a δ value of 1.50 ppm(δ = 90/60 = 450/300 = 1.50). Note that a resonance to the right of TMS has a negative value of δ. Also, since TMS is insoluble in water, other internal standards (δ = 0) are used for this solvent, including the sodium salts of 3-(trimethylsilyl)-1-propanesulfonic acid (also called 4,4-dimethyl-4-silapentane-1-sulfonic acid or DSS) [$(CH_3)_3Si(CH_2)_3SO_3Na$] and 3-(trimethylsilyl)propionic acid [$(CH_3)_3SiCH_2CH_2CO_2Na$].

In the first generation of commercial spectrometers, the range of chemical shifts, such as those in the scale at the bottom of Figures 1.5 and 1.7, was generated by varying the B_0 field while holding the B_1 field, and hence the resonance frequency ν_0, constant. As Eq. (1.3) indicates, an increase in shielding (σ) requires B_0 to be raised in order to keep ν_0 constant. Since nuclei with higher shielding resonate at the right side of the spectrum, the B_0 field in this experiment increases from left to right. Consequently, the right end came to be known as the high field, or upfield, end of the spectrum, and the left end as the low field, or downfield, end. This method was termed *continuous-wave* (CW) *field sweep*. Although the method is rarely used today, its vestigial terms such as "upfield" and "downfield" remain inappropriately in the NMR vocabulary.

Modern spectrometers vary the B_1 frequency, while the B_0 field is kept constant. An increase in shielding (σ) lowers the right side of Eq. (1.3) so that ν_0 must decrease in order to maintain a constant B_0. Thus, the right end of the spectrum, as noted before, corresponds to lower frequencies for more shielded nuclei. The general result is that *frequency increases from right to left and field increases from left to right*. Figure 1.9 summarizes the terminology. The right end of the spectrum still is often referred to as the

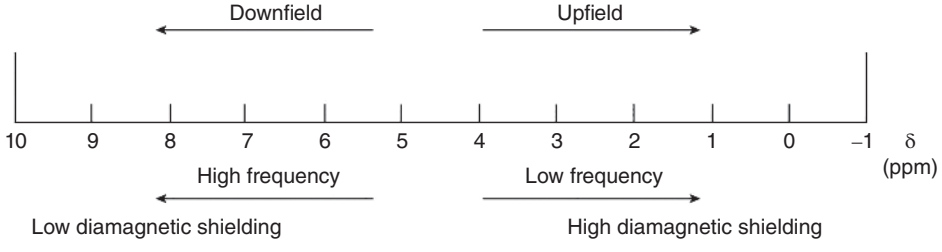

Figure 1.9 Spectral conventions.

high field or upfield end, in deference to the old field-sweep experiment, although it is more appropriate to call it the low-frequency or more shielded end.

The chemical shift is considered further in Chapter 3.

1.3 Excitation and Relaxation

To understand the NMR experiment more fully, it is useful to consider Figure 1.3 again—this time in terms of a collection of nuclei (Figure 1.10). At equilibrium, the $I_z = +½$ nuclei precess around the $+z$-axis, and the $-½$ nuclei precess around the $-z$-axis. Only 20 spins are shown on the surface of the double cone in the figure, and the excess of $+½$ over $-½$ nuclei is exaggerated (12 to 8). The actual ratio of populations of the two states is given by the Boltzmann equation (Eq. (1.1). Inserting the numbers for $B_0 = 7.04$ T yields the result that, for every million spins, there are only about 50 more with $+½$ that $-½$ spin. If the magnetic moments are added vectorially, there is a net vector in the $+z$-direction because of the excess of $+½$ over $-½$ spins. The sum of all the individual spins is called the *magnetization* ($\boldsymbol{M}$). The boldface arrow pointing along the $+z$-direction in Figure 1.10 represents the resultant $\boldsymbol{M}$. Because the spins are distributed randomly (or incoherently) around the z-axis, there is no net x or y magnetization, that is, $M_x = M_y = 0$, and hence, $\boldsymbol{M} = M_z$.

Figure 1.10 also shows the vector that represents the B_1 field placed along the x-axis. When the B_1 frequency matches the Larmor frequency of the nuclei, some $+½$ spins turn over and become $-½$ spins so that M_z decreases slightly. The component of the vector magnetic field ($\boldsymbol{B}$) in the x-direction (B_1) exerts a force on $\boldsymbol{M}$, the result of which is perpendicular to both vectors (inset at lower right of the figure); the force arises from the cross product $\boldsymbol{F} = \boldsymbol{M} \times \boldsymbol{B}$. If B_1 is turned on just briefly, the magnetization vector $\boldsymbol{M}$

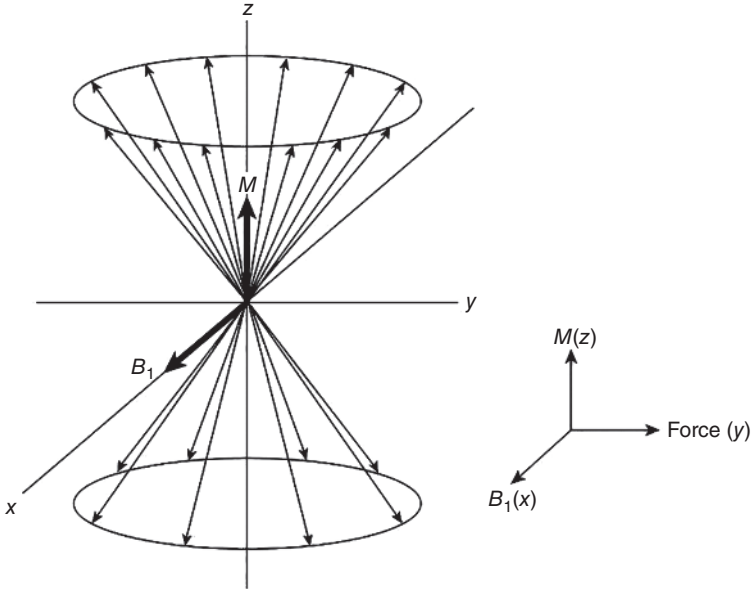

Figure 1.10 Spin-½ nuclei at equilibrium, prior to application of the B_1 field.

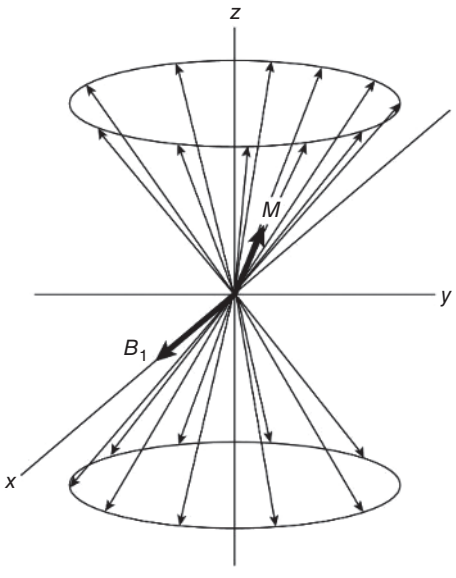

Figure 1.11 Spin-½ nuclei immediately after application of the B_1 field.

tips only slightly off the z-axis, moving toward the y-axis, which represents the mutually perpendicular direction. Figure 1.11 illustrates the result.

The 20 spins of Figure 1.10 include 12 nuclei of spin $+½$ and 8 of spin $-½$. This same set of nuclei, as shown in Figure 1.11, comprise 11 of spin $+½$ and 9 of spin $-½$, after application of the B_1 field. Thus, only one nucleus has changed its spin in this model. The decrease in M_z is exaggerated in the figure, but the tipping of the magnetization vector off the axis is clearly apparent. The positions on the circles, or the *phases*, of the 20 nuclei no longer are random, because the tipping requires bunching of the spins. The phases of the spins now have some *coherence*, and there are x and y components of the magnetization. The xy component of the magnetization is the signal detected electronically as the resonance. It is important to appreciate that the so-called absorption of energy as $+½$ nuclei become $-½$ nuclei is not measured directly.

The B_1 field in Figures 1.10 and 1.11 oscillates back and forth along the x-axis. As Figure 1.12 illustrates from a view looking down the z-axis, B_1 may be considered either (i) to oscillate linearly along the x-axis at so many times per second (with frequency ν) or (ii) to move circularly in the xy plane with angular frequency ω ($2\pi\nu$) in radians per second. The two representations are vectorially equivalent. See Appendix B, and Figure B.1 in particular, for an expansion of these concepts. Resonance occurs when the frequency and phase of B_1 match that of the nuclei precessing at the Larmor frequency.

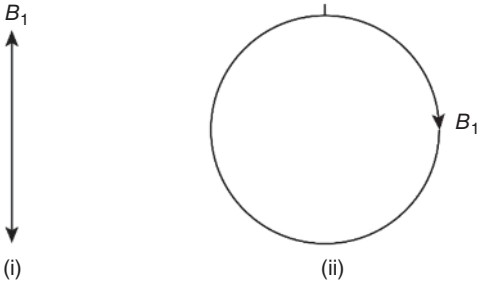

Figure 1.12 Analogy between linearly and circularly oscillating fields.

Figure 1.11 represents a snapshot in time, with the motion of both the B_1 vector and the precessing nuclei frozen. In real time, each nuclear vector is precessing around the z-axis so that the magnetization $\boldsymbol{M}$ also is precessing around that axis. Another way to look at the freeze frame is to consider that the x- and y-axes are rotating at the frequency of the B_1 field. In terms of Figure 1.12, the axes are following the circular motion. Consequently, B_1 appears to be frozen in position along the x-axis, instead of oscillating in the fashions shown in that figure. This *rotating coordinate system* is used throughout the book to simplify magnetization diagrams. In the rotating frame, the individual nuclei and the magnetization $\boldsymbol{M}$ no longer precess around the z-axis but are frozen for as long as they all have the same Larmor frequency as the frequency of the rotating x- and y-axes, corresponding to that of the B_1 field.

Application of B_1 at the resonance frequency results in both energy absorption ($+\frac{1}{2}$ nuclei become $-\frac{1}{2}$) and emission ($-\frac{1}{2}$ nuclei become $+\frac{1}{2}$). Because, initially, there are more $+\frac{1}{2}$ than $-\frac{1}{2}$ nuclei, the net effect is absorption. As B_1 irradiation continues, however, the excess of $+\frac{1}{2}$ nuclei decreases and eventually disappears so that the rates of absorption and emission eventually become equal. Under these conditions, the sample is said to be approaching *saturation*. The situation is ameliorated, however, by natural mechanisms whereby nuclear spins are returned from saturation to equilibrium. Any process that returns the z-magnetization to its equilibrium condition with the excess of $+\frac{1}{2}$ spins is called *spin–lattice*, or *longitudinal*, *relaxation* and is usually a first-order process with time constant T_1 (the time constant is the reciprocal of the rate constant but is the traditional quantity used in this context). For a return to equilibrium, relaxation also is necessary to destroy magnetization created in the xy plane. Any process that returns the x- and y-magnetizations to their equilibrium condition of zero is called *spin–spin*, or *transverse*, *relaxation* and is usually a first-order process with time constant T_2.

Spin–lattice relaxation (T_1) derives primarily from the existence of local oscillating magnetic fields in the sample that correspond to the resonance frequency. The primary source of these random fields is other magnetic nuclei that are in motion. As a molecule tumbles in solution in the B_0 field, each nuclear magnet generates a field caused by its motion. If this field is at the Larmor frequency, excess spin energy of neighboring spins can pass to this motional energy as $-\frac{1}{2}$ nuclei become $+\frac{1}{2}$ nuclei. The resonating spins are relaxed back to their initial state, and the absorption experiment can continue, thereby increasing signal intensity.

For effective spin–lattice relaxation, the tumbling magnetic nuclei must be spatially close to the resonating nucleus. When ^{13}C is under observation, attached protons ($^{13}C—^{1}H$) provide effective spin–lattice relaxation. A carbonyl carbon or a carbon attached to four other carbons thus relaxes very slowly and is more easily saturated because the attached atoms are nonmagnetic (motion of the nonmagnetic nuclei such as ^{12}C and ^{16}O provides no relaxation). Protons are relaxed by their nearest neighbor protons. Thus, protons within CH_2 or CH_3 groups are relaxed by geminal protons (HCH) within the group, but the CH entity must rely on vicinal (CH—CH) or more distant protons.

Spin–lattice relaxation also is responsible for generating the initial excess of $+\frac{1}{2}$ nuclei when the sample is first placed in the probe. In the absence of the B_0 field, all spins have the same magnetic energy. When the sample is immersed in the B_0 field, magnetization begins to build up as spins flip from the effects of interactions with surrounding

magnetic nuclei in motion, eventually creating the equilibrium ratio with an excess of $+\frac{1}{2}$ over $-\frac{1}{2}$ spins.

For x- and y-magnetization to decay toward zero (spin–spin, or T_2, relaxation), the phases of the nuclear spins must become randomized (Figures 1.10 and 1.11). The mechanism that gives the phenomenon its name involves the interaction of two nuclei with opposite spin. The process whereby one spin goes from $+\frac{1}{2}$ to $-\frac{1}{2}$ while the other goes from $-\frac{1}{2}$ to $+\frac{1}{2}$ involves no net change in z-magnetization and hence no spin–lattice relaxation. The switch in spins, however, results in dephasing, because the new spin state has a different phase from the old one. In terms of Figure 1.11, a spin vector disappears from the surface of the upper cone and reappears on the surface of the lower cone (and vice versa) at a new phase position. As this process continues, the phases become randomized around the z-axis, and xy magnetization disappears. This process of two nuclei simultaneously exchanging spins is sometimes called the flip-flop mechanism.

Spin–spin relaxation also arises when the B_0 field is not perfectly homogeneous. Again, in terms of Figure 1.11, if the spin vectors are not located in exactly identical B_0 fields, they differ slightly in Larmor frequencies and hence precess around the z-axis at different rates. As the spins move faster or more slowly relative to each other, eventually their relative phases become randomized. When various nuclei resonate over a range of Larmor frequencies, the line width of the signal naturally increases. The spectral line width at half height and the spin–spin relaxation are related by the expression $w_{1/2} = 1/(\pi T_2)$. Both mechanisms (flip-flop and field inhomogeneity) can contribute to T_2 in the same sample.

The subject of relaxation is discussed further in Section 5.1 and Appendix E.

1.4 Pulsed Experiments

In the pulsed NMR experiment, the sample is irradiated close to the resonance frequency with an intense B_1 field for a very short time. For the duration of the pulse, the $\boldsymbol{B}$ vector on the x-axis (B_1) in the rotating coordinate system exerts a force (see inset in Figure 1.10) on the $\boldsymbol{M}$ vector, which is on the z-axis, pushing the magnetization toward the y-axis. Figures 1.13a,b, respectively, simplify Figures 1.10 and 1.11 by eliminating the individual spins. Only the net magnetization vector $\boldsymbol{M}$ is shown in Figure 1.13.

As long as the strong B_1 field is on, the magnetization vector $\boldsymbol{M}$ continues to rotate, or precess, around B_1 on the x-axis. The strength of the B_1 field is such that, when it is on, it forces precession to occur preferentially around its direction (x), rather than around the natural direction (z) of the weaker B_0 field. Consequently, the primary field present at the nuclei is B_1, so the expression for the precession frequency becomes $\omega = \gamma B_1$. More precisely, this equation holds at the resonance frequency $\omega_0 = \gamma B_0$. Farther and farther from the resonance frequency, the effect of B_1 wanes, and precession around B_0 returns. A full mathematical treatment requires the inclusion of terms in both B_0 and B_1, but, qualitatively, our interest focuses on the events at the resonance frequency.

The angle θ of rotation of the magnetization $\boldsymbol{M}$ increases as long as B_1 is present (Figure 1.13). A short pulse might leave the magnetization at a 30° angle relative to the z-axis (Figure 1.13b). A pulse three times as long (90°) aligns the magnetization along the y-axis (Figure 1.13c). A pulse of double this duration (180°) brings the magnetization along the $-z$-direction (Figure 1.13d), meaning that there is an excess of $-\frac{1}{2}$ spins, or

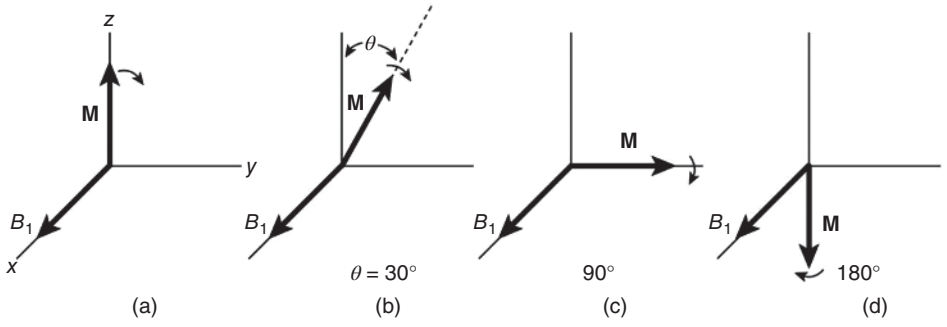

Figure 1.13 (a) Net magnetization ***M*** before application of the B_1 field. (b) After a 30° pulse. (c) After a 90° pulse. (d) After a 180° pulse.

a population inversion, a truly unnatural situation. The exact angle θ caused by a pulse thus is determined by its duration t_p. The angle θ is therefore ωt_p, in which ω is the precession frequency in the B_1 field. Since $\omega = \gamma B_1$, it follows that $\theta = \gamma B_1 t_p$.

If the B_1 irradiation is halted when the magnetization reaches the y-axis (a 90° pulse), and if the magnetization along the y-direction is detected over time at the resonance frequency, then the magnetization would be seen to decay (Figure 1.14). Alignment of the magnetization along the y-axis is a nonequilibrium situation. After the pulse, the x- and y-magnetization (collectively, xy) decays by spin–spin relaxation (T_2). At the same time, z magnetization reappears by spin–lattice relaxation (T_1). The reduction in y magnetization with time shown in the figure is called the *Free Induction Decay* (FID) and is a first-order process with time constant T_2.

The illustration in Figure 1.14 is artificial, because it involves only a single nucleus for which the resonance frequency γB_0 corresponds to the frequency of rotation of the x- and y-axes. Most samples have quite a few different types of protons or carbons so that several resonance frequencies are involved ($\gamma B_0(1 - \sigma_i)$), but the rotating frame can have only a single, or reference, frequency. What happens when there are nuclei with resonance frequencies different from the reference frequency? First, imagine again the case of a single resonance, whose Larmor frequency corresponds to the reference frequency, such as the protons of benzene in Figure 1.5. At the time the 90° B_1 pulse is turned off, the spins are lined up along the y-axis (Figure 1.15a). The nuclei then return to precessing about the z-axis at the Larmor frequency $\omega_0 = \gamma B_0$. In the rotating coordinate system, the x- and y-axes are rotating at γB_0 around the z-axis. Nuclei with the same resonance frequency γB_0 appear not to precess about the z-axis because their frequency of rotation matches that of the rotating frame so that they remain lined up along the z-axis (Figure 1.15a).

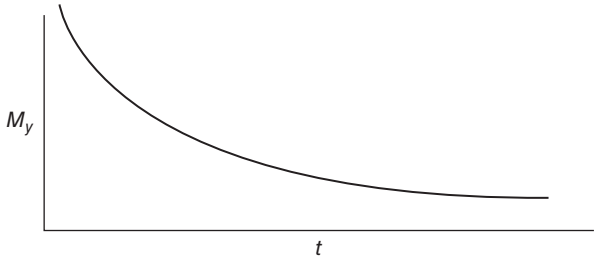

Figure 1.14 Time dependence of the magnetization M_y following a 90° pulse (the free induction decay).

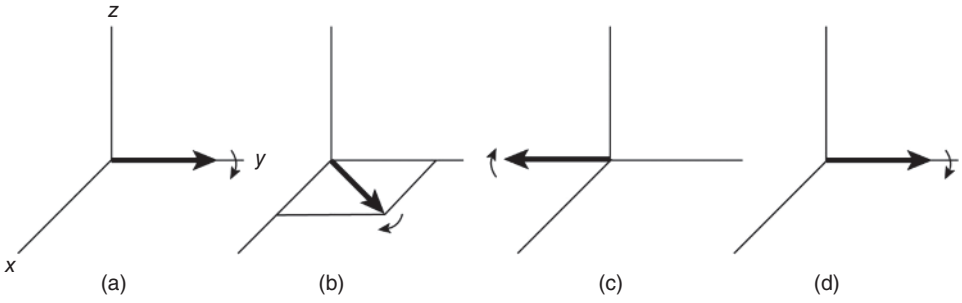

Figure 1.15 Induced magnetization along the *y*-axis as a function of time after a 90° pulse.

In the case of a second nucleus with a different Larmor frequency ($\omega \neq \omega_0 = \gamma B_0$), the nuclear magnets move off the *y*-axis with the *xy* plane (Figure 1.15b). Only nuclei precessing at the reference frequency γB_0 appear to be stationary in the rotating coordinate system. As time progresses, the magnetization continues to rotate within the *xy* plane, reaching the $-y$-axis (Figure 1.15c) and eventually returning to the $+y$-axis (Figure 1.15d). The detected *y*-magnetization during this cycle first decreases and then falls to zero as it passes the $y = 0$ point. Next it moves to a negative value in the $-y$-region (Figure 1.15c), and finally returns to positive values (Figure 1.15d). The magnitude of the magnetization thus varies periodically like a cosine function. When it is again along the $+y$-axis (Figure 1.15d), the magnetization is slightly smaller than at the beginning of the cycle, because of spin–spin relaxation (T_2). Moreover, it has moved out of the *xy* plane (not shown in the figure) as *z*-magnetization returns through spin–lattice relaxation (T_1). The magnetization varies as a cosine function with time, continually passing through a sequence of events illustrated by Figure 1.15.

Figure 1.16a shows what the FID looks like for the protons of acetone, when the reference frequency ω_0 is not the same as the Larmor frequency ω of acetone. The horizontal distance between adjacent maxima is the reciprocal of the difference between the Larmor frequency ω of acetone and the B_1 frequency ω_0 ($(\Delta\omega)^{-1} = (\omega - \omega_0)^{-1}$). The intensities of the maxima decrease as *y* magnetization is lost through spin–spin relaxation. Because the line width of the spectrum is determined by T_2, the FID contains all the necessary information to display a spectrum: frequency, line width, and overall intensity.

Now consider the case of two nuclei with different resonance frequencies, each different from the reference frequency. Their decay patterns are superimposed, reinforcing, and interfering to create a complex FID, as in Figure 1.16b for the protons of methyl acetate [$CH_3(C{=}O)OCH_3$]. By the time there are four frequencies, as in the carbons of 3-hydroxybutyric acid [$CH_3CH(OH)CH_2CO_2H$] shown in Figure 1.16c, it is impossible to unravel the frequencies visually. The mathematical process called Fourier analysis matches the FID with a series of sinusoidal curves and exponential functions to obtain from them the frequencies, line widths, and intensities of each component. The FID is a plot in time (see Figures 1.14 and 1.16), so the experiment is said to occur in the *time domain*. The experimentalist, however, wants a plot of frequencies, so the spectrum must be transformed to a *frequency domain,* as shown in Figures 1.5 and 1.7. The Fourier transformation (FT) from time to frequency domain is carried out rapidly and automatically by computer, and the experimentalist does not need to examine the FID.

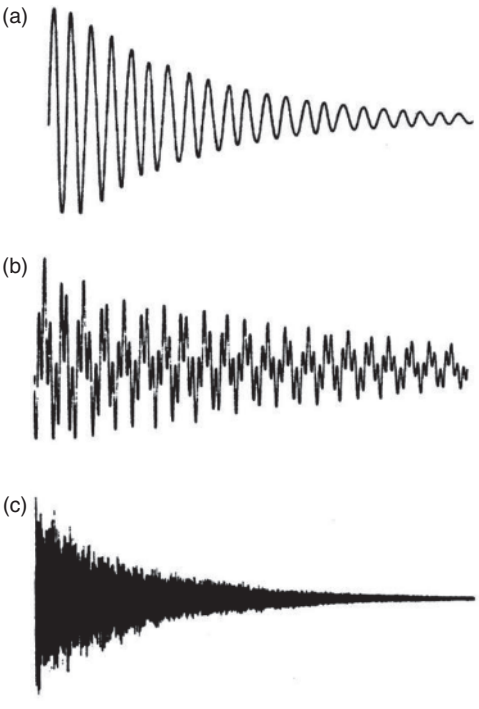

Figure 1.16 The free induction decay for the ^{1}H spectra of (a) acetone and (b) methyl acetate. (c) The free induction decay for the ^{13}C spectrum of 3-hydroxybutyric acid. All samples are without solvent.

1.5 The Coupling Constant

The form of a resonance can be altered by the presence of a distinct, neighboring magnetic nucleus. In 1-chloro-4-nitrobenzene (**1.1**),

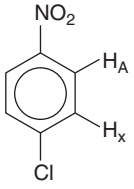

1.1

for example, there are two types of protons, labeled A and X, which are, respectively, ortho to nitro and ortho to chloro. For the time being, we will ignore any effects from the identical A and X protons across the ring. Each proton has a spin of ½ and therefore can exist in two I_z spin states, $+½$ and $-½$, which differ in population only in parts per million. Almost exactly half the A protons have $+½$ X neighbors, and half have $-½$ X neighbors. The magnetic environments provided by these two types of X protons are not identical, so the A resonance is split into two peaks (Figures 1.17a and 1.18). By the same token, the X nucleus exists in two distinct magnetic environments, because the A proton has two unequal spin states. The X resonance also is split into two peaks for the same reasons (Figures 1.17b and 1.18). Quadrupolar nuclei, such as those of the chlorine and nitrogen atoms in molecule **1.1**, often act as if they are nonmagnetic and

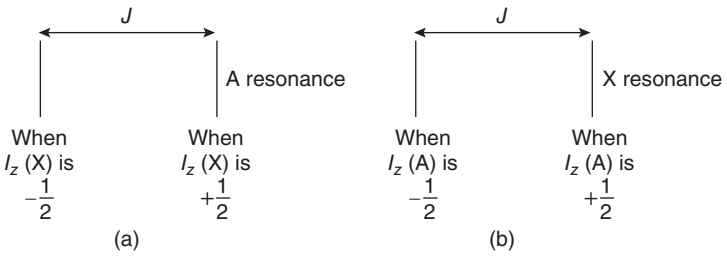

Figure 1.17 The four peaks of a first-order, two-spin system (AX): (a) the A portion and (b) the X portion.

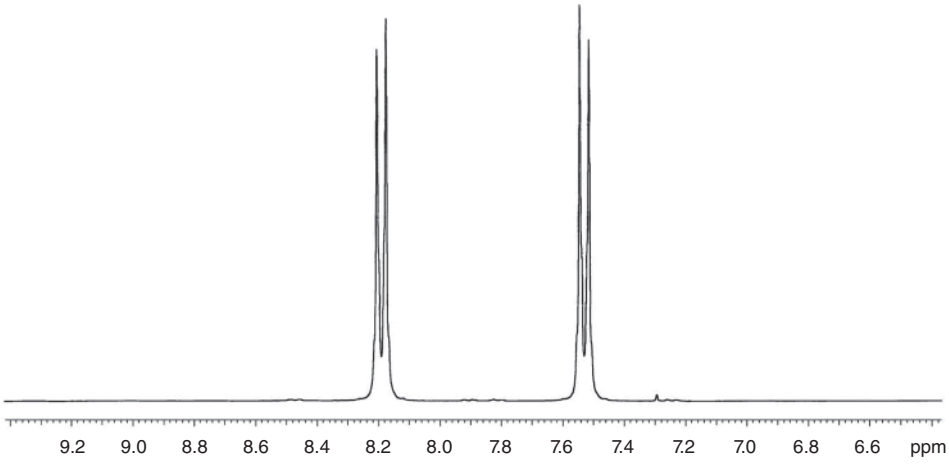

Figure 1.18 The 300 MHz ^{1}H spectrum of 1-chloro-4-nitrobenzene in $CDCl_3$.

may be ignored in this context. Thus, the proton resonance of chloroform ($CHCl_3$) is a singlet; the proton resonance is not split by chlorine. This phenomenon is considered in detail in Section 5.1.

The influence of neighboring spins on the multiplicity of peaks is called *spin–spin splitting*, *indirect coupling*, or *J-coupling*. The distance between the two peaks for the resonance of one nucleus split by another is a measure of how strongly the nuclear spins influence each other and is called the *coupling constant J*, measured in the energy unit Hz. In 1-chloro-4-nitrobenzene (**1.1**), the coupling between A and X is 10.0 Hz, a relatively large value of *J* for two protons. In general, when there are only two nuclei in the coupled system, the resulting spectrum is referred to as AX. Notice that the splitting in both the A and the X portions of the spectrum is the same (Figure 1.18), since *J* is a measure of the interaction between the nuclei and must be identical for both nuclei. Moreover, *J* is independent of B_0, because the magnitude of the interaction depends only on nuclear properties and not on external quantities such as the field. Thus, in 1-chloro-4-nitrobenzene (**1.1**), *J* is 10.0 Hz when measured either at 7.05 T (300 MHz, Figure 1.18) or at 14.1 T (600 MHz).

For two nuclei to couple, there must be a mechanism whereby information about spin is transferred between them. The most common such mechanism involves the interaction of electrons along the bonding path between the nuclei (see Figure 1.19 for an

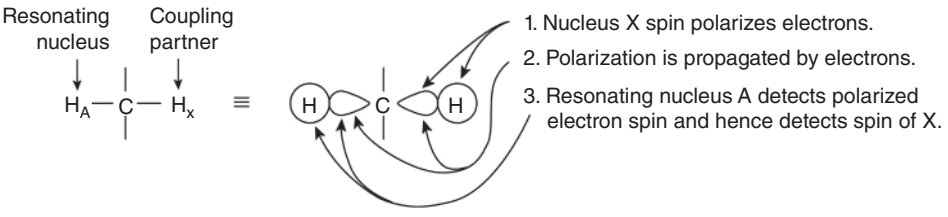

Figure 1.19 The mechanism for indirect spin–spin coupling.

abbreviated coupling pathway over two bonds). In the same fashion as protons, electrons act like spinning particles and have a magnetic moment. The X proton (H_X) influences, or polarizes, the spins of its surrounding electrons, making the electron spins favor one I_z state very slightly. Thus, a proton of spin $+\frac{1}{2}$ polarizes the electron to $-\frac{1}{2}$. The electron in turn polarizes the other electrons of the C—H bond, and so on, finally reaching the resonating A proton (H_A). This mechanism is discussed further in Section 4.3. Because the nuclei do not interact directly but via the electron pathway, the interaction is called *indirect coupling*. As an interaction through bonds, it is a useful parameter in drawing conclusions about molecular bonding, such as bond order and stereochemistry.

Additional splitting occurs when a resonating nucleus is close to more than one nucleus. For example, 1,1,2-trichloroethane (**1.2**)

$$ClCH_2^A—CH^XCl_2$$

1.2

has two types of protons, which we label H_A (CH_2) and H_X (CH). The A protons are subject to two different environments, from the $+\frac{1}{2}$ and $-\frac{1}{2}$ spin states of H_X, and therefore are split into a 1 : 1 doublet, analogous to the situations shown in Figures 1.17 and 1.18. The X proton, however, is subject to *three* different magnetic environments, because the spins of H_A must be considered collectively: both may be $+\frac{1}{2}$ (++), both may be $-\frac{1}{2}$ (−−), and one may be $+\frac{1}{2}$, while the other is $-\frac{1}{2}$, for which there are two equivalent possibilities, (+−) and (−+). The three different A environments—(++), ((+−)/(−+)), and (−−)—therefore result in three X peaks in the ratio 1 : 2 : 1 (Figure 1.20). Thus, the spectrum of **1.2** contains a 1 : 1 doublet and a 1 : 2 : 1 triplet and is referred to as A_2X (or AX_2 if the labels are switched) (Figure 1.21). The value of J is found in three different spacings in the spectrum between any two adjacent peaks of either multiplet (Figures 1.20 and 1.21).

As the number of neighboring spins increases, so does the complexity of the spectrum. The two identical ethyl groups in diethyl ether form an A_2X_3 spectrum (Figure 1.22). The methyl protons are split into a 1 : 2 : 1 triplet by the neighboring methylene protons, as in the X resonance of Figure 1.20. Because the methylene protons are split by three methyl protons, there are four peaks in the methylene resonance. The neighboring methyl protons can have all positive spins (+++), two positive spins and one negative (in three ways: ++−, +−+, and −++), one positive spin and two negative (also in three ways: +−−, −+−, and −−+), or all spins negative (−−−). The result is a 1 : 3 : 3 : 1 quartet (Figure 1.23). The triplet–quartet pattern seen in Figure 1.22 is a reliable and general indicator for the presence of an ethyl group.

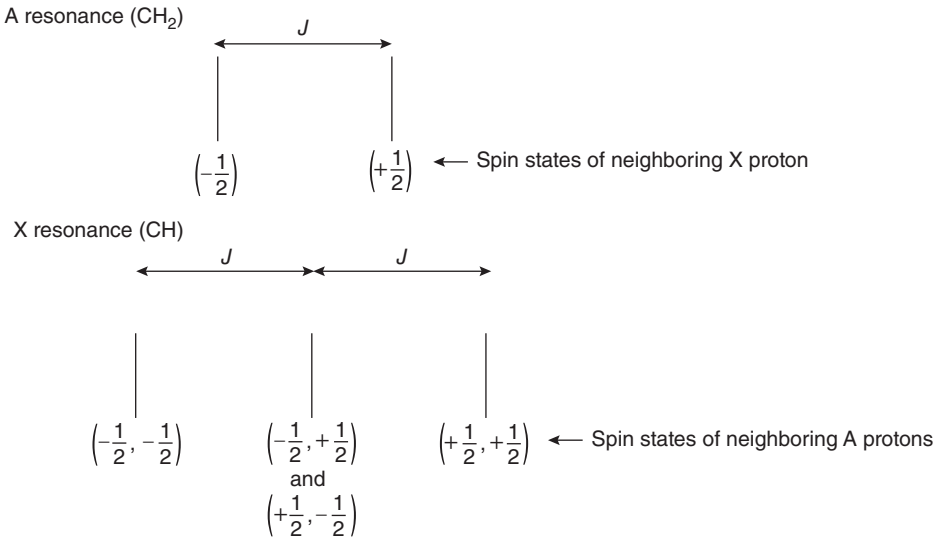

Figure 1.20 The five peaks of a first-order, three-spin system (A_2X).

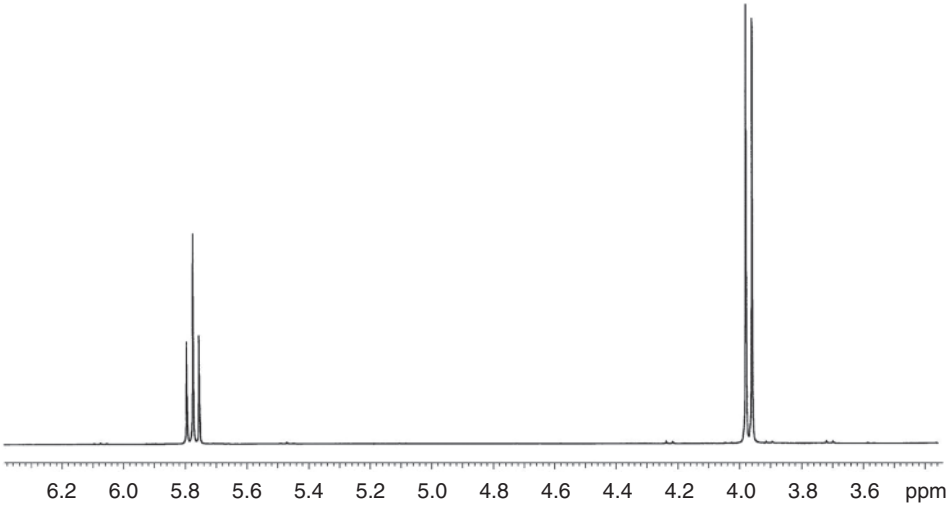

Figure 1.21 The 300 MHz ^{1}H spectrum of 1,1,2-trichloroethane in $CDCl_3$.

The splitting patterns of larger spin systems may be deduced in a similar fashion. If a nucleus is coupled to n equivalent nuclei with $I = ½$, there are $n + 1$ peaks, unless second-order effects, discussed in Chapter 4, are present. The intensity ratios, to a first-order approximation, correspond to the coefficients in the binomial expansion and may be obtained from Pascal's triangle (Figure 1.24), since arrangements of the two I_z states are statistically independent events. Pascal's triangle is constructed by summing two horizontally adjacent integers and placing the result one row lower and between the two integers. Zeros are imagined outside the triangle. The first row (1) gives the resonance multiplicity (an unsplit singlet) when there is no neighboring spin,

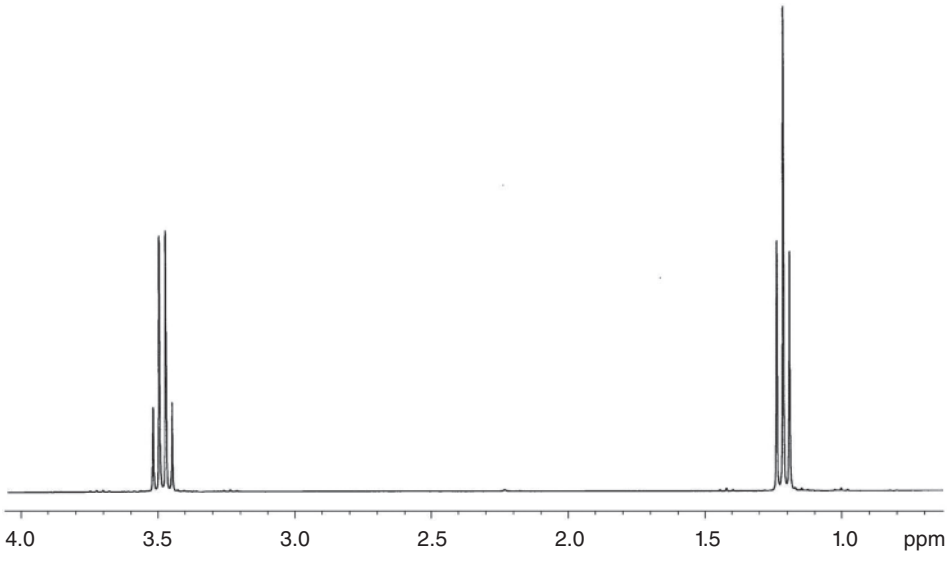

Figure 1.22 The 300 MHz ^{1}H spectrum of diethyl ether in $CDCl_3$.

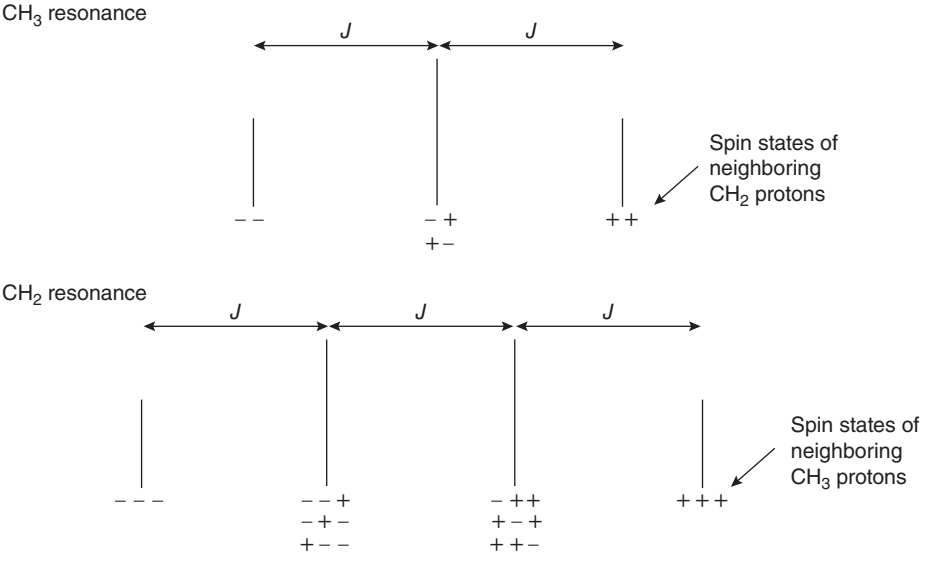

Figure 1.23 The seven peaks of the first-order A_2X_3 spectrum.

the second row (1 : 1) gives the multiplicity when there is one neighboring spin, and so on. We already have seen that two neighboring spins give a 1 : 2 : 1 triplet and three give a 1 : 3 : 3 : 1 quartet, as shown, respectively, in the third and fourth rows of Pascal's triangle (Figure 1.24). Four neighboring spins are present for the CH proton in the arrangement —CH_2—CHX—CH_2— (X is nonmagnetic), and the CH resonance is a 1 : 4 : 6 : 4 : 1 (the fifth row) quintet (AX_4). The CH resonance from an isopropyl

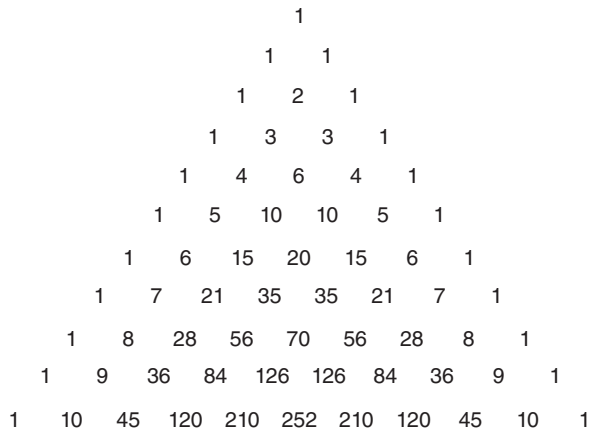

Figure 1.24 Pascal's triangle.

Table 1.1 Common first-order spin–spin splitting patterns.

Spin system	Molecular substructure	A multiplicity	X multiplicity
AX	$—CH^A—CH^X—$	Doublet (1 : 1)	Doublet (1 : 1)
AX_2	$—CH^A—CH_2^X—$	Triplet (1 : 2 : 1)	Doublet (1 : 1)
AX_3	$—CH^A—CH_3^X$	Quartet (1 : 3 : 3 : 1)	Doublet (1 : 1)
AX_4	$—CH_2^X—CH^A—CH_2^X—$	Quintet (1 : 4 : 6 : 4 : 1)	Doublet (1 : 1)
AX_6	$CH_3^X—CH^A—CH_3^X$	Septet (1 : 6 : 15 : 20 : 15 : 6 : 1)	Doublet (1 : 1)
A_2X_2	$—CH_2^A—CH_2^X—$	Triplet (1 : 2 : 1)	Triplet (1 : 2 : 1)
A_2X_3	$—CH_2^A—CH_3^X$	Quartet (1 : 3 : 3 : 1)	Triplet (1 : 2 : 1)
A_24	$—CH_2^X—CH_2^A—CH_2^X—$	Quintet (1 : 4 : 6 : 4 : 1)	Triplet (1 : 2 : 1)

group, $—CH(CH_3)_2$, is a 1 : 6 : 15 : 20 : 15 : 6 : 1 (the seventh row) septet (AX_6). Several common spin systems are given in Table 1.1.

Except in cases of second-order spectra (Sections 4.1 and 4.7), coupling between protons that have the same chemical shift does not lead to splitting in the spectrum. It is for this reason that the spectrum of benzene in Figure 1.1 is a singlet, even though each proton is coupled to its two ortho neighbors. For the same reason, protons within a methyl group normally do not cause splitting of the methyl resonance. Other examples of unsplit spectra (singlets) include those of acetone, cyclopropane, and dichloromethane. The absence of splitting between coupled nuclei with identical resonance frequencies is quantum mechanical in nature and is explained in Appendix C.

Almost all the coupling examples given so far have been between vicinal protons, over three bonds (H—C—C—H). Coupling over four or more bonds usually is small or unobservable. It is possible for geminal protons ($—CH_2—$) to split each other, provided that each proton of the methylene group has a different chemical shift. Such geminal splittings are observed when the carbon is part of a ring with unsymmetrical substitution on the upper and lower faces ($—CH_2—CXY—$), when there is a single chiral center in the

molecule (—CH_2—CXYZ), or when an alkene lacks an axis of symmetry (CH_2=CXY). Such couplings are discussed further in Sections 4.2 and 4.4.

Coupling can occur between ^1H and ^{13}C, as well as between two protons. Because ^{13}C is in such low natural abundance (about 1.1%), these couplings are not important in analyzing ^1H spectra. In 99 cases out of 100, protons are attached to nonmagnetic ^{12}C atoms. Small satellite peaks from the 1.1% of ^{13}C sometimes can be seen in ^1H spectra. In the ^{13}C spectrum, the carbon nuclei are coupled to nearby protons. The largest couplings occur with protons that are directly attached to the carbon. Thus, the ^{13}C resonance of a methyl carbon is split into a quartet, that of a methylene carbon into a triplet, and that of a methine carbon (CH) into a doublet. A quaternary carbon lacks an attached proton and hence does not exhibit a one-bond coupling. Figure 1.25a shows the ^{13}C spectrum of 3-hydroxybutyric acid ($CH_3CH(OH)CH_2CO_2H$), which contains a carbon resonance with each type of multiplicity. From right to left are seen a quartet (CH_3), a triplet (CH_2),

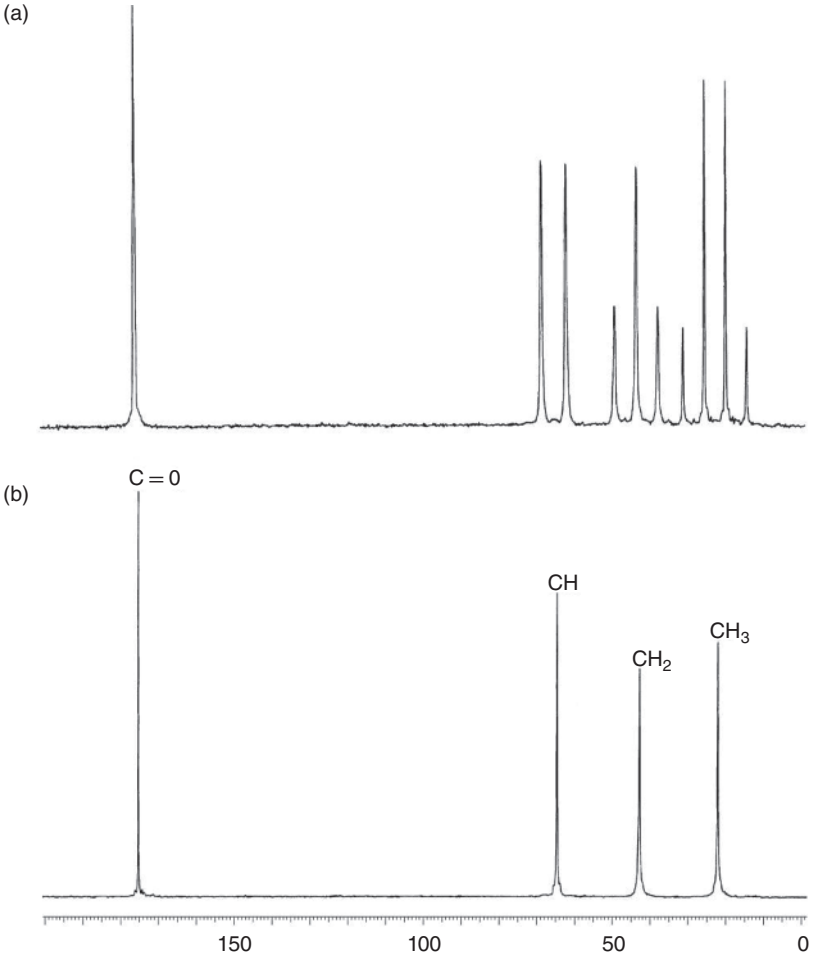

Figure 1.25 (a) The 22.6 MHz ^{13}C spectrum of 3-hydroxybutyric acid, $CH_3CH(OH)CH_2CO_2H$, without solvent. (b) The ^{13}C spectrum of the same compound with proton decoupling.

a doublet (CH), and a singlet (CO_2H). Thus, the splitting pattern in the ^{13}C spectrum is an excellent indicator of each of these types of groupings within a molecule.

Instrumental procedures, called *decoupling*, are available by which spin–spin splittings may be removed. These methods, discussed in Section 5.3, involve irradiating one nucleus with an additional field (B_2) while observing another nucleus resonating in the B_1 field. Because a second field is being applied to the sample, the experiment is called *double resonance*. This procedure was used to obtain the ^{13}C spectrum of methyl acetate in Figure 1.7b and the spectrum of 3-hydroxybutyric acid at the bottom of Figure 1.25. It is commonly employed to obtain a very simple ^{13}C spectrum, in which each carbon gives a singlet. Measurement of both decoupled and coupled ^{13}C spectra then produces in the first case, a simple picture of the number and types of carbons and in the second case, the number of protons to which they are attached (Figure 1.25). Coupling is treated in more detail in Chapter 4.

1.6 Quantitation and Complex Splitting

The signal that is detected when nuclei resonate is directly proportional to the number of spins present. Thus, the protons of a methyl group (CH_3) produce three times the signal of a methine proton (CH). This difference in intensity can be measured through electronic integration and exploited to elucidate molecular structure. Figure 1.26 illustrates electronic integration for the ^1H spectrum of ethyl *trans*-crotonate ($CH_3CH{=}CH(CO)OCH_2CH_3$). The vertical displacement of the continuous line above or through each resonance provides a relative measure of the area under the peaks. The vertical displacements show that the doublet at δ 5.84, the quartet at δ 4.19, and

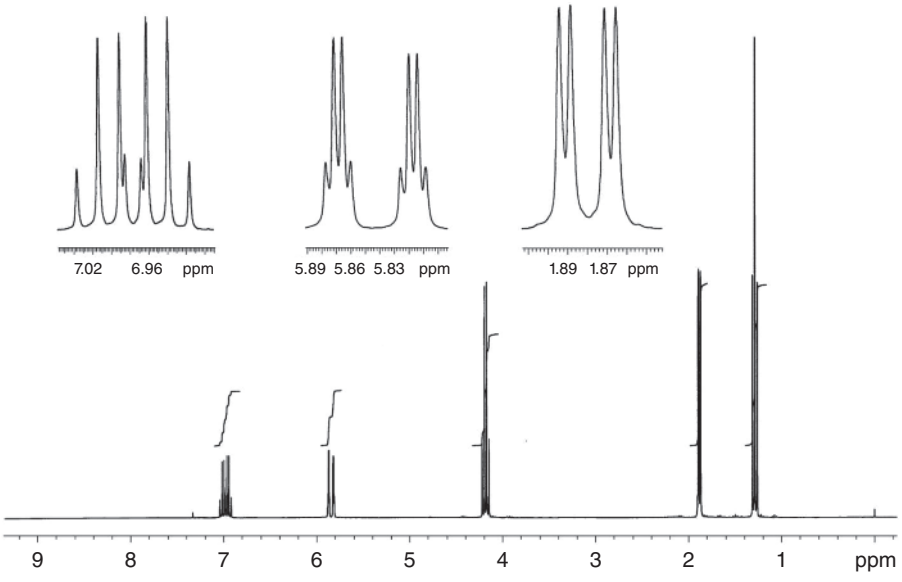

Figure 1.26 The 300 MHz ^1H spectrum of ethyl *trans*-crotonate ($CH_3CH{=}CH(CO)OCH_2CH_3$) in $CDCl_3$. The upper multiplets are expansions of three resonances. The continuous lines above or through a resonance is its integral.

the triplet at δ 1.28 are, respectively, in the ratio 1 : 2 : 3. Quantitative integrals are provided digitally by the spectrometer. The integration provides only relative intensity data, however, so that the experimentalist must select a resonance with a known or suspected number of protons and normalize the other integrals to it.

Each of the peaks in the ^{1}H spectrum of ethyl crotonate illustrated in Figure 1.26 may be assigned by examining the integrals and splitting patterns. The triplet at the lowest frequency (the highest field, δ 1.28) has a relative integral of 3 and must come from the methyl part of the ethyl group. Its J value corresponds to that of the quartet in the middle of the spectrum at δ 4.19, whose integral is 2. This latter multiplet then must come from the methylene group. The mutually coupled methyl triplet and methylene quartet form the resonances for the ethyl group attached to oxygen (—OCH_2CH_3). The methylene resonance is at a higher frequency than the methyl resonance because CH_2 is closer than CH_3 to the electron-withdrawing oxygen atom.

The remaining resonances in the spectrum come from protons coupled to more than one type of proton. Coupling patterns in such cases are more complex, as seen in the three spectral expansions in Figure 1.26. The highest-frequency (lowest-field) resonance (δ 6.98) has an intensity of unity and comes from one of the two alkenic (—CH=) protons. This resonance is split into a doublet (J = 16 Hz) by the other alkenic proton, and then each member of the doublet is further split into a quartet (J = 7 Hz) by coupling to the methyl group on carbon with a crossover of the inner two peaks. Stick diagrams (often called a tree) are useful in analyzing complex multiplets, as in Figure 1.27, for the resonance at δ 6.98.

The resonance of unit integral at δ 5.84 is from the other alkenic proton and is split into a doublet (J = 16 Hz) by the proton at δ 6.98. There is a small coupling (1 Hz) over four bonds to the methyl group, giving rise to a quartet (Figure 1.28). The significance of these differences in the magnitude of couplings is discussed in Chapter 4. The resonance at δ 6.98 can be recognized as originating from the proton closer to the methyl group. Thus J is larger because it is over three, rather than four, bonds.

The resonance at δ 1.88 has an integral of 3 and hence comes from the remaining methyl group, attached to the double bond. Because it is split by both of the alkenic protons, but with unequal couplings (7 and 1 Hz), four peaks result (Figure 1.29). This grouping is called a *doublet of doublets*; the term *quartet* normally is reserved for 1 : 3 : 3 : 1 multiplets. The two unequal couplings in the resonance at δ 1.88 correspond precisely to the quartet splittings found, respectively, in the two alkenic resonances.

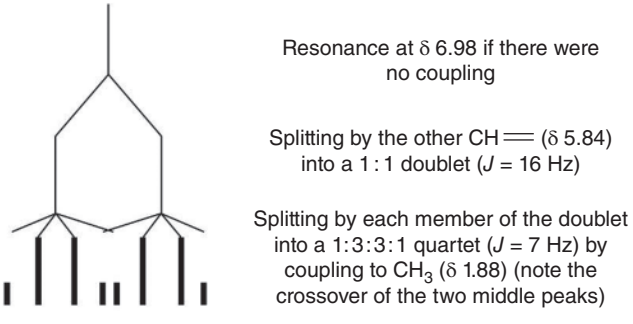

Figure 1.27 Overlapping peaks of the resonance δ 6.98, which arise when nuclei are unequally coupled to more than one other set of spins.

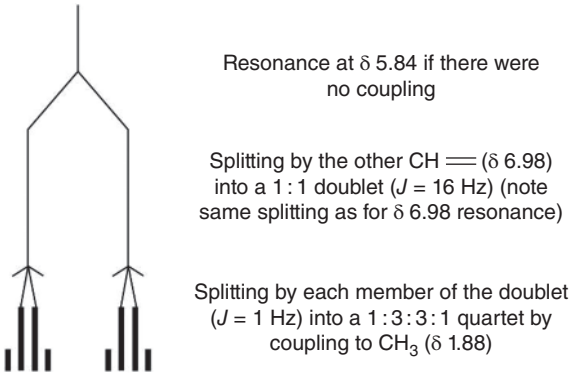

Figure 1.28 Overlapping peaks of the resonance at δ 5.84 (not to scale).

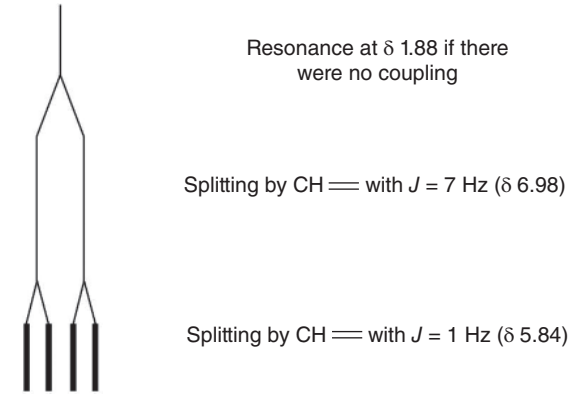

Figure 1.29 Overlapping peaks of the resonance at δ 1.88 (not to scale).

The final assignments are as follows:

δ 1.9 7.0 5.8 4.2 1.3

$CH_3CH_2{=}CHCO_2CH_2CH_3$

Integration also may be used as a measure of the relative amounts of the components of a mixture. In this case, after normalizing for the number of protons in a grouping, the proportions of the components may be calculated from the relative integrals of protons in different molecules. An internal standard with a known concentration may be included. Comparisons of other resonances with those of the standard then can provide a measure of the absolute concentration.

1.7 Commonly Studied Nuclides

Which nuclei (in this context, "nuclides") are useful in chemical problems? The answer depends on one's area of specialty. Certainly, for the organic chemist, the most important elements are carbon, hydrogen, oxygen, and nitrogen. The biochemist would add phosphorus to the list. The organometallic or inorganic chemist would focus on whichever elements are of potential use in a particular subfield, possibly boron, silicon, tin, mercury, platinum, or some of the low-intensity nuclei, such as iron and potassium.

Table 1.2 NMR properties of common nuclei.

Nuclide	Spin	Natural abundance (N_a)(%)	Natural sensitivity (N_s) (for equal numbers of nuclei) (vs ^{1}H)	Receptivity (vs ^{13}C)	NMR frequency (at 7.05 T)	Reference substance
Proton	1/2	99.985	1.00	5680	300.00	$(CH_3)_4Si$
Deuterium	1	0.015	0.00965	0.0082	46.05	$(CD_3)_4Si$
Lithium-7	3/2	92.58	0.293	1540	38.86	LiCl
Boron-10	3	19.58	0.0199	22.1	32.23	$Et_2O \cdot BF_3$
Boron-11	3/2	80.42	0.165	754	96.21	$Et_2O \cdot BF_3$
Carbon-13	1/2	1.108	0.0159	1.00	75.45	$(CH_3)_4Si$
Nitrogen-14	1	99.63	0.00101	5.69	21.69	$NH_3(1)$
Nitrogen-15	1/2	0.37	0.00104	0.0219	30.42	$NH_3(1)$
Oxygen-17	5/2	0.037	0.0291	0.0611	40.68	H_2O
Fluorine-19	1/2	100	0.833	4730	282.27	CCl_3F
Sodium-23	3/2	100	0.0925	525	79.36	NaCl (aq)
Aluminum-27	5/2	100	0.0206	117	78.17	$Al(H_2O)_6^{3+}$
Silicon-29	1/2	4.70	0.00784	2.09	59.61	$(CH_3)_4Si$
Phosphorus-31	1/2	100	0.0663	377	121.44	85% H_3PO_4
Sulfur-33	3/2	0.76	0.00226	0.0973	23.04	CS_2
Chlorine-35	3/2	75.53	0.0047	20.2	29.40	NaCl (aq)
Chlorine-37	3/2	24.47	0.00274	3.8	24.47	NaCl (aq)
Potassium-39	3/2	93.1	0.000509	2.69	14.00	K^+
Calcium-43	7/2	0.145	0.00640	0.0527	20.19	$CaCl_2$ (aq)
Iron-57	1/2	2.19	0.0000337	0.0042	9.71	$Fe(CO)_5$
Cobalt-59	7/2	100	0.277	1570	71.19	$K_3Co(CN)_6$
Copper-63	3/2	69.09	0.0931	365	79.58	$Cu(C_3CN)_4^+ BF_4^-$
Selenium-77	1/2	7.58	0.00693	2.98	57.22	$Se(CH_3)_2$
Rhodium-103	1/2	100	0.0000312	0.177	9.56	Rh metal
Tin-119	1/2	8.58	0.0517	25.2	37.29	$(CH_3)_4Sn$
Tellurium-125	1/2	7.0	0.0315	12.5	78.51	$Te(CH_3)_2$
Platinum-195	1/2	33.8	0.00994	19.1	64.38	Na_2PtCl_6
Mercury-199	1/2	16.84	0.00567	5.42	53.73	$(CH_3)_2Hg$
Lead-207	1/2	22.6	0.00920	11.8	62.57	$Pb(CH_3)_4$

Source: For a more complete list, see Ref. [1].

The success of the experiment depends on several factors, which are listed in Table 1.2 for a variety of nuclides and are described in the following sections:

Spin. The overall spin of a nucleus (second column in Table 1.2) is determined by the spin properties of the protons and neutrons, as discussed in Section 1.1. By and large, spin-½ nuclei exhibit more favorable NMR properties than quadrupolar nuclei

($I > 1/2$). Nuclei with odd mass numbers have half-integral spins ($1/2$, 3/2, etc.), whereas those with even mass and odd charge have integral spins (1, 2, etc.). Quadrupolar nuclei have a unique mechanism for relaxation that can result in extremely short relaxation times, as is discussed in Section 5.1. The relationship between lifetime (Δt) and energy (ΔE) is given by the Heisenberg uncertainty principle: $\Delta E \Delta t \geq \hbar$ (the normal statement of this principle in terms of position and momentum can be converted to this expression in terms of energy and time through conversion of units). When the lifetime of the spin state, as measured by the relaxation time, is very short, the larger uncertainty in energies (ΔE) implies a larger band of frequencies (Δt), or a broadened signal, in the NMR spectrum. The relaxation time, and hence the broadening of the spectral lines, also depends on the distribution of charge within the nucleus, as determined by the quadrupole moment. For example, quadrupolar broadening makes ^{14}N ($I = 1$) a generally less useful nucleus than ^{15}N ($I = 1/2$), even though ^{14}N is far more abundant.

Natural abundance. Nature provides us with nuclides in varying amounts (third column in Table 1.2). Whereas ^{19}F and ^{31}P are 100% abundant and ^{1}H nearly so, ^{13}C is present only to the extent of 1.1%. The most useful nitrogen (^{15}N) and oxygen (^{17}O) nuclides occur to the extent of much less than 1%. The NMR experiment naturally is easier with nuclides with higher natural abundance. Because so little ^{13}C is present, there is a very small probability of having two ^{13}C atoms at adjacent positions in the same molecule ($0.011 \times 0.011 = 0.00\,012$, or about 1 in 10 000). Thus, *J*-couplings are not easily observed between two ^{13}C nuclei in ^{13}C spectra, although procedures to measure them have been developed.

Natural sensitivity. Nuclides have differing sensitivities to the NMR experiment (fourth column in Table 1.2), as determined by the gyromagnetic ratio γ and the energy difference ΔE ($= \gamma \hbar B_0$) between the spin states (Figure 1.6). The larger the energy difference, the more nuclei are present in the lower spin state (see Eq. (1.1)), and hence the more are available to absorb energy. With its large γ, the proton is one of the most sensitive nuclei, whereas ^{13}C and ^{15}N, unfortunately, are rather weak (Figure 1.6). Tritium (^{3}H) is useful to the biochemist as a radioactive label. It has $I = 1/2$ and is highly sensitive. Since it has zero natural abundance, it must be introduced synthetically. As a hydrogen label, deuterium also is useful, but it has very low natural sensitivity and a spin $I = 1$ and also must be introduced synthetically. Nuclei that are of interest to the inorganic chemist vary from poorly sensitive, such as iron and potassium, to highly sensitive, such as lithium and cobalt. Thus, it is important to be familiar with the natural sensitivity of a nucleus before designing an NMR experiment.

Receptivity. The intensity of the signal for a spin-$1/2$ nucleus is determined by both the natural abundance (in the absence of synthetic labeling) and the natural sensitivity of the nuclide. The mathematical product of these two factors is a good measure of how amenable a specific nucleus is to the NMR experiment. Because chemists are quite familiar with the ^{13}C experiment, the product of natural abundance and natural sensitivity for a nucleus is divided by the product for ^{13}C to give the factor known as the *receptivity* (fifth column in Table 1.2). Thus, the receptivity of ^{13}C is, by definition, 1.00. The ^{15}N experiment then is seen to be about 50 times less sensitive than that for ^{13}C, since the receptivity of ^{15}N is 0.0219. In addition to these factors, Table 1.2 also contains the NMR resonance frequency at 7.05 T (the sixth column). The last column contains the reference substance for each nuclide, for which in most cases $\delta = 0$.

1.8 Dynamic Effects

According to the principles outlined in the previous sections, the ^1H spectrum of methanol (CH_3OH) should contain a doublet of integral 3 for the CH_3 group (coupled to OH) and a quartet of integral 1 for the OH group (coupled to CH_3). Under conditions of high purity or low temperature, such a spectrum is observed (Figure 1.30b). The presence of a small amount of an acidic or basic impurity, however, can catalyze the intermolecular exchange of the hydroxyl proton. When this proton becomes detached from the molecule by any mechanism, information about its spin states is no longer available to the rest of the molecule. For coupling to be observed, the rate of exchange must be considerably slower than the magnitude of the coupling, in Hz (s^{-1}). Thus, a proton could exchange a few times per second and still maintain coupling. If the rate of exchange is faster than *J,* no coupling is observed between the hydroxyl proton and the methyl protons. Hence, at high temperatures (Figure 1.30a), the ^1H spectrum of methanol contains only two singlets. If the temperature is lowered or the amount of acidic or basic catalyst is decreased, the exchange rate slows down. The coupling constant continues to be absent until the exchange rate reaches a critical value at which the proton resides sufficiently long on oxygen to permit the methyl group to detect the spin states. As can be seen from the figure, the transition from *fast exchange* (upper) to *slow exchange* (lower) can be accomplished for methanol over a temperature range of 80 °C. Under most spectral conditions, minor amounts of acid, or base impurities are present, so hydroxyl protons do not usually exhibit couplings to other nuclei. The integral is still unity for the OH group, because the amount of catalyst is small. Sometimes the exchange rate is intermediate, between fast and slow exchange, and broadened peaks are observed. Amino (NH or NH_2), ammonium (H_3N^+), and thiol (SH) protons exhibit similar behavior.

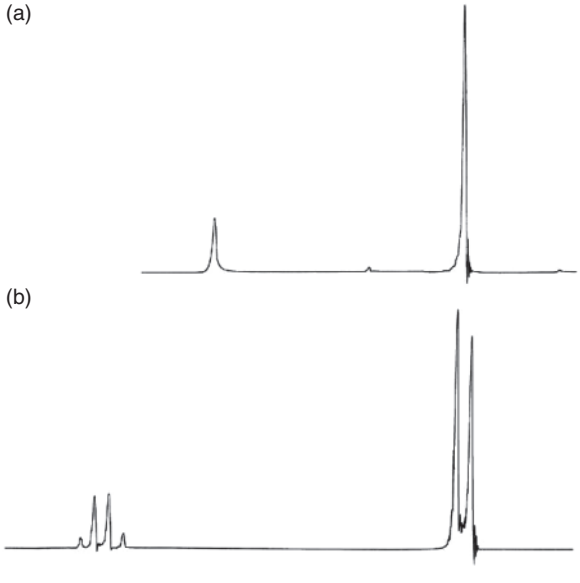

Figure 1.30 The 60 MHz ^1H spectrum of CH_3OH at +50 °C (a) and at −30 °C (b).

A process that averages coupling constants also can average chemical shifts. A mixture of acetic acid and benzoic acid can contain only one ^1H resonance for the CO_2H groups from both molecules. The carboxyl protons exchange between molecules so rapidly that the spectrum exhibits only the average of the two. Moreover, when the solvent is water, exchangeable protons such as OH in carboxylic acids or alcohols do not give separate resonances. Thus, the ^1H spectrum of acetic acid (CH_3CO_2H) in water contains two, not three, peaks: the water and carboxyl protons appear as a single resonance whose chemical shift falls at the weighted average of those of the pure materials. If the rate of exchange between —CO_2H and water could be slowed sufficiently, separate resonances would be observed. Carboxyl protons give separate resonances in organic solvents such as $CDCl_3$. In dry dimethyl sulfoxide (DMSO, usually deuterated, as in $(CD_3)_2SO$) exchange often is slow enough to give separate resonances when there are multiple hydroxyl groups in the molecule and even exhibit H—O—C—H vicinal couplings).

Intramolecular (unimolecular) reactions also can influence the appearance of the NMR spectrum if the rate is comparable to that of chemical shift differences. The molecule cyclohexane [$(CH_2)_6$], for example, contains distinct axial and equatorial protons, yet the spectrum exhibits only one sharp singlet at room temperature. There is no splitting, because all protons have the same average chemical shift. Flipping of the ring interconverts the axial and equatorial positions. When the rate of this process is greater (in s^{-1}) than the chemical-shift difference between the axial and equatorial protons (in Hz, which, of course, is s^{-1}), the NMR experiment does not distinguish the two types of protons, and only one peak is observed. Again, this situation is called fast exchange. At lower temperatures, however, the process of ring flipping is much slower. At −100 °C, the NMR experiment can distinguish the two types of protons, so two resonances are observed (slow exchange). At intermediate temperatures, broadened peaks are observed that reflect the transition from fast to slow exchange. Figure 1.31 illustrates the spectral changes as a function of temperature for cyclohexane, in which all protons but one have been replaced by deuterium to remove vicinal proton–proton couplings to simplify the spectrum (**1.3**, in which the lone hydrogen on the left is axial and the lone hydrogen on the right is equatorial).

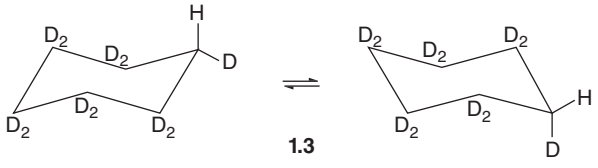

Processes that bring about averaging of spectral features occur reversibly, whether by acid-catalyzed intermolecular exchange as in methanol or by unimolecular reorganization as in cyclohexane. NMR is one of the few methods able to examine effects of reaction rates when a system is at equilibrium. Most other kinetic methods require that one substance be transformed irreversibly into another. The dynamic effects of the averaging of chemical shifts or coupling constants provide a nearly unique window into processes that occur on the order of a few times per second. The subject is examined further in Section 5.2.

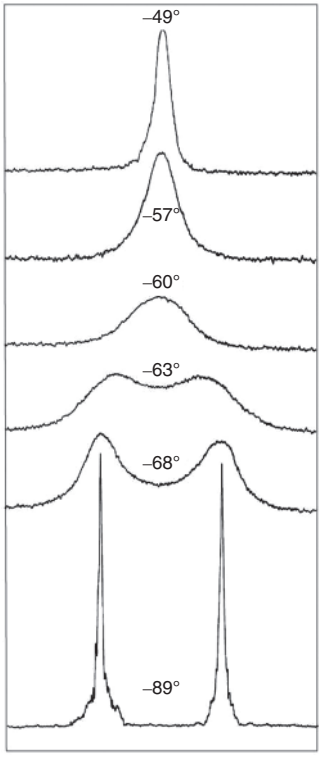

Figure 1.31 The 60 MHz ^{1}H spectrum of cyclohexane-d_{11} as a function of temperature. Source: Bovey et al. 1964 [2]. Reproduced with permission from American Institute of Physics.

1.9 Spectra of Solids

All of the examples and spectra illustrated thus far have been for liquid samples. Certainly, it would be useful to be able to take NMR spectra of solids, so why have we avoided discussing such samples? Under conditions normally used for liquids, the spectra of solids are broad and unresolved, providing only modest amounts of information. There are two primary reasons for the poor resolution of solid samples. In addition to the indirect spin–spin (J) interaction that occurs between nuclei through bonds, nuclear magnets also can couple through the direct interaction of their nuclear dipoles. This *dipole–dipole*, *dipolar*, *direct*, or *D-coupling* occurs through space, rather than through bonds. The resulting coupling is designated with the letter D and is much larger than J-coupling.

In solution, dipoles are continuously reorienting themselves through molecular tumbling. Just as two bar magnets have no net interaction when averaged over all mutual orientations, two nuclear magnets have no net dipolar interaction because of the randomizing effect of tumbling. Thus, the D-coupling normally averages to zero in solution. The indirect J-coupling does not average to zero, because tumbling cannot average out an interaction that takes place through bonds. In the solid phase, however, nuclear dipoles are held rigidly in position so that the D-coupling does not average to zero. The dominant interaction between nuclei in solids is, in fact, the D-coupling, which is on the order of several hundred to a few thousand hertz. Dipolar interactions also can become apparent in the spectra of very large biological molecules, which move very slowly in solution. The magnitude of the interaction depends on the angle between the nuclear dipoles. Each dipole can assume any relative angle in the solid, so the actual value of the

dipolar coupling varies from zero to the maximum value in the optimal arrangement for a solid sample. Since such interactions assume a range of values, are much larger than *J*-coupling and most chemical shifts, and do not average out, very broad signals are produced.

As with the *J*-coupling, the *D*-coupling may be eliminated by the application of a strong B_2 field. Power levels required for the removal of *D* must be much higher than those for *J* decoupling, since *D* is 2–3 orders of magnitude larger than *J*. High-powered decoupling is used routinely to reduce the line width of the spectra of solids. In practice, dipolar decoupling is most easily brought about between different spin-½ nuclei, as when ^{13}C is observed with decoupling of ^{1}H. The analogous all-proton experiment is more difficult, since both observed and irradiated nuclei have the same frequency range. Thus, the acquisition of solid-state ^{13}C spectra is much simpler than that of ^{1}H spectra. Quadrupolar nuclei such as ^{27}Al also are more difficult to observe in the solid.

The second factor that contributes to line broadening for solids is *chemical shielding anisotropy*. The term "chemical shift anisotropy" should be avoided in this context, since, strictly speaking, the chemical shift is a scalar quantity and cannot be anisotropic. In solution, the observed chemical shift is the average of the shielding of a nucleus over all orientations in space, as the result of molecular tumbling. In a solid, shielding of a specific nucleus in a molecule depends on the orientation of the molecule with respect to the B_0 field. Consider the carbonyl carbon of acetone. When the B_0 field is parallel to the C=O bond, the nucleus experiences a different shielding from when the B_0 field is perpendicular to the C=O bond (Figure 1.32). The ability of electrons to circulate and give rise to shielding varies according to the arrangement of bonds in space. Differences between the abilities of electrons to circulate in the arrangements shown in the figure, as well as in all other arrangements, generate a range of shieldings and hence a range of resonance frequencies. Such anisotropy is largest for unsaturated carbons (C=O, C=C). For saturated carbons, shielding is similar for most orientations in the field, so anisotropy is low.

Double irradiation does not average chemical shielding anisotropy, since the effect is entirely geometrical. The problem is largely removed by spinning the sample to mimic the process of tumbling. The effects of spinning are optimized when the axis of spin is set at an angle of 54°74′ to the direction of the B_0 field. This is the angle between the edge of a cube and the adjacent solid diagonal. Spinning of a cube along this diagonal averages each Cartesian direction by interconverting the *x*-, *y*-, and *z*-axes, just as tumbling in solution does. When the sample is spun at that angle to the field, the various arrangements of Figure 1.32 average, and the chemical shieldings are reduced to the isotropic chemical shift. The technique therefore has been called *Magic Angle Spinning* (MAS). Because shielding anisotropies are generally a few hundred to several thousand hertz, the rate of spinning must exceed this range in order to average all orientations. Typical

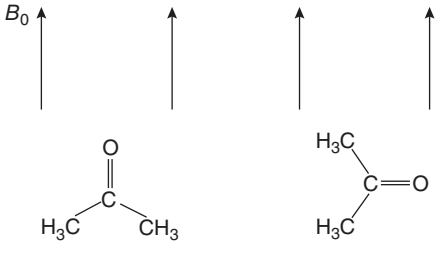

Figure 1.32 Anisotropy of shielding in the solid state.

minimum spinning rates are 2–5 kHz, but rates up to 50 kHz are possible. Spinning at the magic also reduces dipolar and quadrupolar interactions.

The combination of strong irradiation to reduce dipolar couplings and MAS to eliminate shielding anisotropy results in ^{13}C spectra of solids that are almost as high in resolution as those of liquids. Spectra of protons or of quadrupolar nuclei in a solid can be obtained but require more complex experiments. Figure 1.33 shows the ^{13}C spectrum of polycrystalline β-quinol methanol clathrate. The broad, almost featureless spectrum at the top (Figure 1.33a) is typical of solids. Strong double irradiation (Figure 1.33b) reduces dipolar couplings and brings out some features. MAS in addition to decoupling (Figure 1.33c) produces a truly high-resolution spectrum.

Relaxation times are extremely long for nuclei in the solid state because the motion necessary for spin–lattice relaxation is slow or absent. Carbon-13 spectra could take a very long time to record because the nuclei must relax for several minutes between pulses. The problem is solved by taking advantage of the more favorable properties of the protons that are coupled to the carbons. The same double irradiation process that eliminates *J*- and *D*-couplings is used to transfer some of the proton's higher magnetization and faster relaxation to the carbon atoms. The process is called *cross polarization* (CP) and is standard for most solid spectra of ^{13}C. After the protons are moved onto the *y*-axis by a 90° pulse, a continuous *y* field is applied to keep the magnetization precessing about that axis, a process called *spin locking*. The frequency of this field ($\gamma_H B_H$) is controlled by the spectrocopist. When the ^{13}C channel is turned on, its frequency ($\gamma_C B_C$) can be set to equal the ^{1}H frequency (the *Hartmann–Hahn condition*, $\gamma_H B_H = \gamma_C B_C$). Both protons and carbons then are precessing at the same frequency and hence have the same net magnetization, which, for carbon, is increased over that used in the normal pulse experiment. Carbon resonances thus have enhanced intensity and faster (proton-like) relaxation. When carbon achieves maximum intensity, B_C is turned off (ending the *contact time*) and carbon magnetization is acquired, while B_H is retained for dipolar decoupling and other beneficial effects.

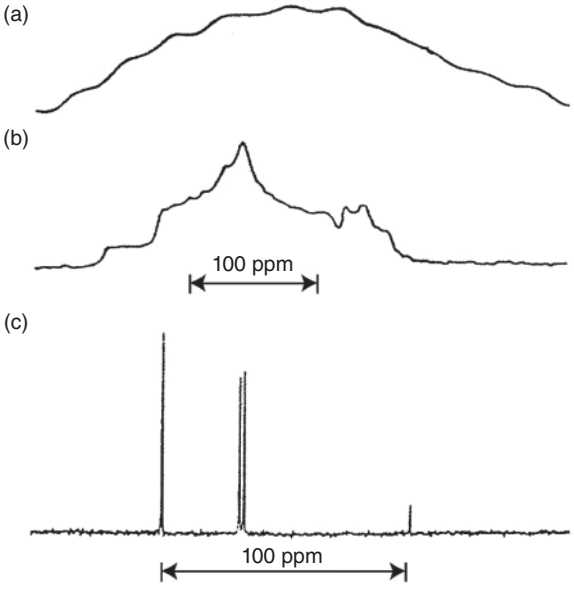

Figure 1.33 The ^{13}C spectrum of polycrystalline β-quinol methanol clathrate (a) without dipolar decoupling, (b) with decoupling, and (c) with both decoupling and magic angle spinning. Source: Terao 1983 [3]. Reproduced with permission from JEOL News.

The higher resolution and sensitivity of the experiment with cross polarization and magic angle spinning (CP/MAS) opened vast new areas to NMR investigations. Inorganic and organic materials that do not dissolve could be subjected to NMR analysis. Synthetic polymers and coal were two of the first materials to be examined. Biological and geological materials, such as wood, humic acids, and biomembranes, became general subjects for NMR study. Problems unique to the solid state—for example, structural and conformational differences between solids and liquids—also may be examined.

Problems

In the following problems, assume fast rotation around all single bonds.

1.1 Determine the number of chemically different hydrogen atoms and their relative proportions in the following molecules. Do the same for carbon atoms.

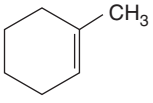

(a)

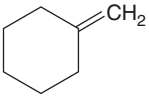

(b)

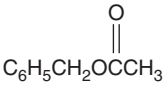

(c)

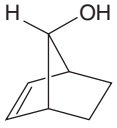

(d)

1.2 What is the expected multiplicity for each proton resonance in the following molecules?

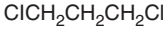

(a)

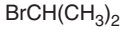

(b)

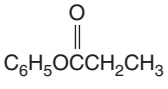

(c)

(d)

1.3 Predict the multiplicities for the ^{1}H and the ^{13}C resonances in the absence of decoupling for each of the following compounds. For the ^{13}C spectra, give only the multiplicities caused by coupling to attached protons. For the ^{1}H spectra, give only the multiplicities caused by couplings to vicinal protons (HCCH).

(a)

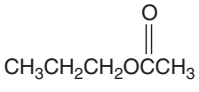

(b)

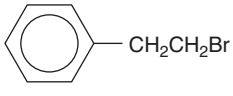

(c)

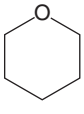

(d)

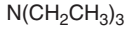

(e)

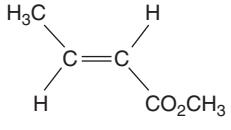

1.4 For each of the following 300 MHz ^{1}H spectra, carry out the following operations. (i) From the elemental formula, calculate the unsaturation number

U (= C + 1 − ½(X − N), in which U is the number of unsaturations (1 for a double bond, 2 for a triple bond, and 1 for each ring), C is the number of tetravalent elements (C, Si, etc.), X is the number of monovalent elements (H and the halogens), and N is the number of trivalent elements (N, P, etc.)). (ii) Calculate the relative integrals for each group of protons. Then convert the integrals to absolute numbers by selecting one group to be of a known integral. (iii) Assign a structure to the compound. Be sure that your structure agrees with the spectrum in all aspects: number of different proton groups, integrals, and splitting patterns.

(a) C_4H_9Br

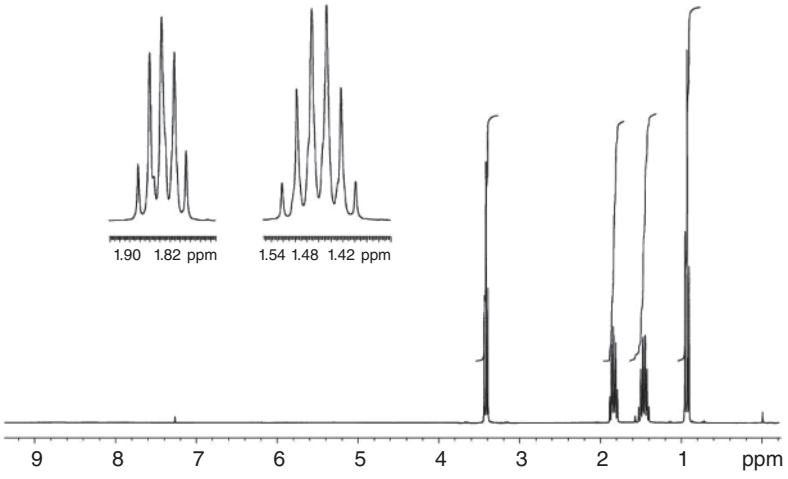

(b) $C_7H_{16}O_3$ (The resonance at δ 1.2 is a 1 : 2 : 1 triplet and that at δ 3.6 is a 1 : 3 : 3 : 1 quartet.)

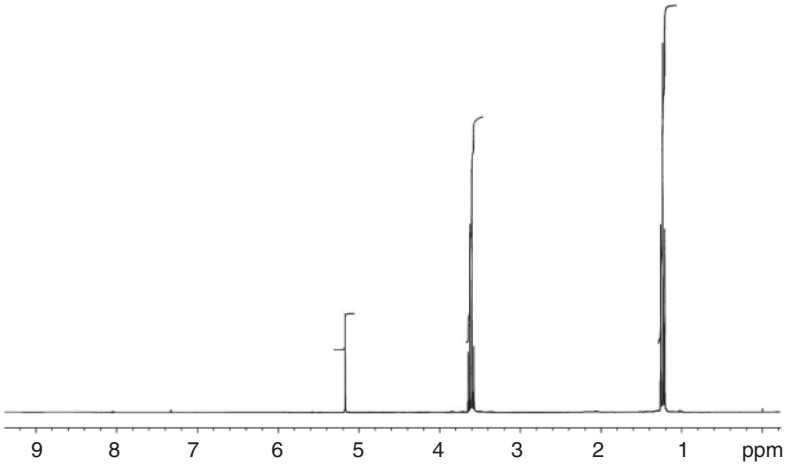

(c) $C_5H_8O_2$ (Ignore stereochemistry at this stage.)

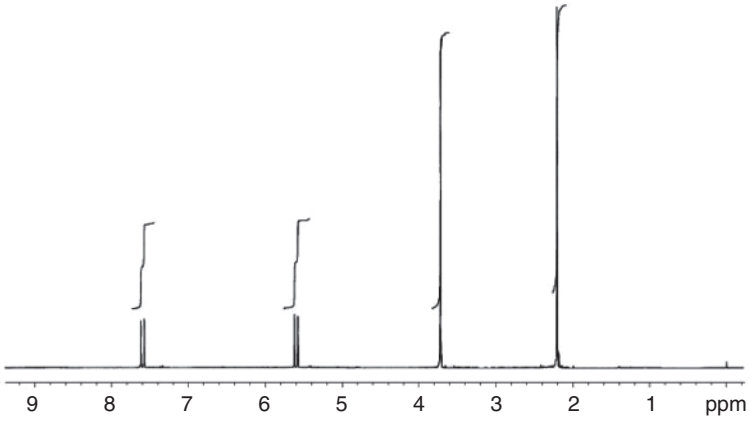

(d) $C_9H_{11}O_2N$ (*Hint:* The highest-frequency resonances (δ 6.6–7.8) come from a *para*-disubstituted phenyl ring. They are doublets. The resonance at δ 4.3 is a quartet, and that at δ 1.4 is a triplet.)

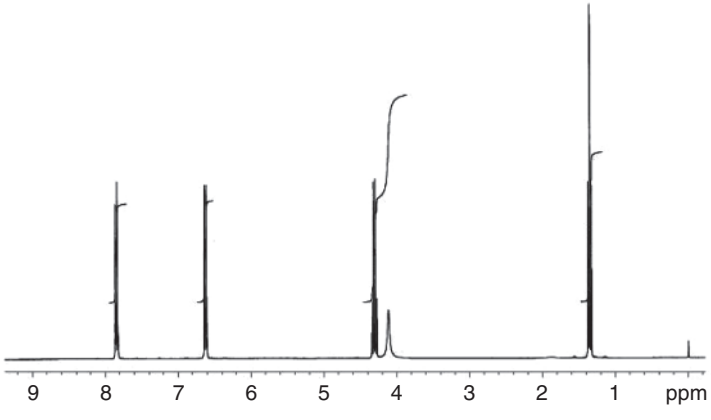

(e) C_5H_9ON (The resonances at δ 1.2 and 2.6 are triplets.)

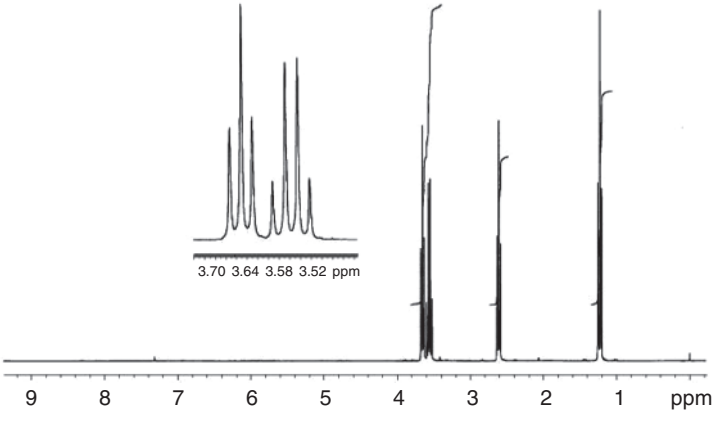

Tips on Solving NMR Problems

Spoiler alert: Some of these tips may be used directly in solving the foregoing problems and therefore should be studied only after you have made every effort to complete the problems. Many of these tips anticipate material that is covered in Chapters 3 and 4.

1) The elemental formula of a compound is obtained only rarely from elemental analysis. Usually, it is obtained from high-resolution mass spectrometric experiments. Often, the information is not available and must be inferred from the NMR spectra. The ^{13}C spectrum, for example, provides a reasonable count of all carbon atoms, and the relative amounts of equivalent carbons. As carbon functionalities are deduced from the NMR spectrum, they should be written down for later assembly of the entire molecule out of its constituents. Evidence for heteroatoms is obtained from mass spectrometry and from an analysis of chemical shifts.
2) If the elemental formula is provided in a problem, the first step is to calculate the unsaturation number as given in Problem 1.4. As unsaturations are deduced during analysis of the NMR spectra, they should be enumerated and compared with the unsaturation number until all are accounted for.
3) Upon completion of a problem, double check that every chemical shift, coupling constant, and integral is in agreement with the concluded structure.
4) The first overview of the ^{1}H spectrum should determine whether there are aromatics, alkenes, and saturated functionalities (with and without electron-withdrawing groups). A similar overview of the ^{13}C spectrum should indicate whether there are carbonyl groups. The spectral ranges for these classes of functionalities are developed in Chapter 3.
5) For a given type of substituent X, methyl groups (CH_3—X) are found at the lowest frequency (highest field), followed by methylene groups (—CH_2—X) and methinyl groups (>CH—X), both in ^{1}H and ^{13}C spectra.
6) Ethyl groups are indicated by a 1 : 2 : 1 triplet and a 1 : 3 : 3 : 1 quartet with a common coupling constant, when isolated from coupling with other groups. Isopropyl groups are indicated by a 1 : 1 doublet and a 1 : 6 : 15 : 20 : 15 : 6 : 1 septet. Sometimes the smallest peaks at either end of the septet are too small to be observed, so the resonance at first glance resembles a quintet.
7) Electron-withdrawing groups such as NO_2, Cl, Br, OH, CN, NH_2, (C=O)R, CHO, CO_2H, and C=C shift saturated ^{1}H and ^{13}C resonances according to their respective electronegativities. Throughout this text, the letter R is considered to be an alkyl substituent, whereas Ar is used for an aromatic substituent. The effect is attenuated rapidly with distance so that in 1-bromopropane ($BrCH_2CH_2CH_3$), for example, the effect is largest for the nearest hydrogen or carbon and decreases thereafter.
8) Unsaturated (NO_2, CN, C=O) or lone-pair-bearing (R_2N:, RO:, Cl:) substituents attached to double bonds and aromatic rings exert resonance effects that can shift alkenic and aromatic resonances to either higher or lower frequency, depending on whether the effect is electron withdrawal (unsaturated substituents) or election donation (lone-pair-bearing substituents) by resonance. Aromatic groups as substituents may be either electron withdrawing or electron donating. The effect of alkyl substituents R is described in Tip 5.

9) Primary ethers (CH_2—OR) and alcohols (CH_2—OH) are found typically at around δ 3.7, with secondary cases (CH—O) at higher frequency and methyl cases (CH_3—O) at lower frequency, in line with Tip 5. Primary amines (CH_2N) are found typically at around δ 2.7 with the appropriate variations for secondary and methyl cases. Methyls next to carbonyl groups are found at about δ 2.1, and those next to double bonds with only hydrocarbon substituents are at about δ 1.7.
10) Cyclopropane methylene protons (C—CH_2—C) are found at the lowest frequency (highest field) of any hydrocarbon, usually at about δ 0.2. Cyclopropane methine protons (C—CHR—C) are not normally in this region.
11) Ester methylene groups [R(C=O)—O—CH_2] are found at higher frequency (δ c. 4.2) than corresponding ether or alcohol methylene groups (δ c. 3.7) because the ester oxygen is more electron withdrawing. Resonance withdrawal by the carbonyl group places a formal positive charge on the ester oxygen [$(RC—O^-)=O^+—CH_2$].
12) Aldehyde protons [H(C=O)] resonate at a nearly unique position near δ 9.8.
13) Carboxyl protons [HO(C=O)] resonate at the very high frequency range of δ 12–14. Consequently, they may be out of the normally observed range of δ 0–10. If a carboxyl group is suspected, the spectral width should be adjusted accordingly. A wide range of δ −1 to +15 should include all resonances, in the absence of paramagnetic impurities. For ^{13}C, a window of δ −5 to +225 similarly should be inclusive.
14) Protons on nitrogen or oxygen in amines and alcohols (OH, NH, NH_2) are usually observed in chloroform solution as broad, unsplit peaks in the range δ 1–4, because of exchange phenomena. In organic solvents such as $CDCl_3$, the range is δ 1–2 for dilute alcohols (ROH), but at higher concentrations or without solvent, the peak moves to δ 3–5. Phenols (ArOH) resonate at δ 5–7 in $CDCl_3$ and δ 9–11 in DMSO.
15) Exchangeable protons may be identified by adding a drop of D_2O to a chloroform solution. Two layers are formed, with the small aqueous layer on top. The tube is shaken, and the OH and NH protons exchange with D_2O and become OD and ND, which are not observed in the spectrum. Thus the spectrum is recorded before and after addition of the drop of D_2O, and resonances from exchangeable protons disappear. The aqueous layer at the top should be out of the receiver coils and not detected.
16) The $n+1$ rule for identifying the number of neighboring protons has limited utility. Currently, proton connectivities are more likely to be determined by the two-dimensional correlation spectroscopy (COSY) experiment (Chapter 6) and carbon substitution patterns (CH_3 vs CH_2 vs CH vs C) by the distortionless enhancement by polarization transfer (DEPT) or related experiments (Chapter 5).

References

1.1 Lambert, J.B. and Riddell, F.G. (1983). *The Multinuclear Approach to NMR Spectroscopy*. Dordrecht: D. Reidel.
1.2 Bovey, F.A., Hood, F.P. III, Anderson, E.W., and Kornegay, R.L. (1964). *J. Chem. Phys.* 41: 2042.
1.3 Terao, T. (1983). *JEOL News* 19: 12.

Further Reading

Abraham, R.J., Fisher, J., and Loftus, P. (1992). *Introduction to NMR Spectroscopy*. New York: Wiley.

Becker, E.D. (2000). *High Resolution NMR*, 3e. New York: Academic Press.

Bovey, F.A., Jelinski, L.W., and Mirau, P.A. (1988). *Nuclear Magnetic Resonance Spectroscopy*, 2e. San Diego: Academic Press.

Breitmaier, E. (2002). *Structure Elucidation by NMR in Organic Chemistry: A Practical Guide*, 3e. New York: Wiley.

Brevard, C. and Granger, P. (1981). *Handbook of High Resolution Multinuclear NMR*. New York: Wiley.

Brey, W.S. (ed.) (1988). *Pulse Methods in 1D and 2D Liquid-Phase NMR*. New York: Academic Press.

Claridge, T.D.W. (2016). *High-Resolution NMR Techniques in Organic Chemistry*, 3e. New York: Elsevier.

Derome, A.E. (1987). *Modern NMR Techniques*. Oxford, UK: Pergamon Press.

Duddeck, H. and Dietrich, W. (1992). *Structure Elucidation by Modern NMR*, 2e. New York: Springer Verlag.

Farrar, T.C. (1989). *Pulse Nuclear Magnetic Resonance Spectroscopy*, 2e. Chicago: Farragut Press.

Field, L.D. and Sternhell, S. (ed.) (1989). *Analytical NMR*. Chichester, UK: Wiley.

Findeisen, M. and Berger, S. (2014). *50 and More Essential NMR Experiments: A Detailed Guide*. New York: Wiley-VCH.

Freeman, R. (1988). *A Handbook of Nuclear Magnetic Resonance*. New York: Longman Scientific & Technical.

Friebolin, H. (2011). *Basic One- and Two-Dimensional NMR Spectroscopy*, 5e. New York: Wiley-VCH.

Fyfe, C.A. (1983). *Solid State NMR for Chemists*. Guelph, ON: C.F.C. Press.

Günther, H. (2013). *NMR Spectroscopy*, 3e. New York: Wiley.

Harris, R.K. (1983). *Nuclear Magnetic Resonance Spectroscopy*. London: Pitman Publishing Ltd.

Harris, R.K. and Wasylishen, R.E. (ed.) (2012). *Encyclopedia of NMR* (10 volume set). New York: Wiley.

Hore, P.J. (2015). *Nuclear Magnetic Resonance*, 2e. New York: Oxford University Press.

Jackman, L.M. and Sternhell, S. (1969). *Applications of Nuclear Magnetic Resonance Spectroscopy in Organic Chemistry*, 2e. Oxford, UK: Pergamon Press.

Laws, D.D., Bitter, H.-M.L., and Jerschow, A. (ed.) (2002). *Angew. Chem. Int. Ed.* 41: 3096–3129.

Ning, Y.-C. and Ernst, R.R. (2005). *Structural Identification of Organic Compounds with Spectroscopic Techniques*. Weinheim, Germany: Wiley-VCH.

Sanders, J.K.M. and Hunter, B.K. (1993). *Modem NMR Spectroscopy*, 2e. Oxford: Oxford University Press.